Acceleration scaling and stochastic dynamics of a fluid particle in turbulence

Rémi Zamansky [*]

Institut de Mécanique des Fluides de Toulouse (IMFT), Université de Toulouse,
CNRS-INPT-UPS, 31400 Toulouse, France

It is well known that the fluid-particle acceleration is intimately related to the dissipation rate of turbulence, in line with the Kolmogorov assumptions. However, various experimental and numerical works have reported as well its dependence on the kinetic energy, which is generally attributed to intermittency and nonindependence of the small-scale dynamics from large-scale ones. The analyses given in this paper focus on statistics of the fluid-particle acceleration conditioned on both the local dissipation rate and the kinetic energy. It is shown that this quantity presents an exponential dependence on the kinetic energy with a growth rate independent of the Reynolds number, in addition to the expected power-law behavior with the dissipation rate. The exponential growth, which clearly departs from the previous propositions, reflects additional kinematic effects of the flow structures on the acceleration. Regarding intermittency, to account for the persistence of the effect of the large scales on the dissipation rate, it is further proposed scaling laws for the Reynolds number dependence of the conditional and unconditional acceleration variance using Barenblatt's incomplete similarity framework. It is then shown that both these intermittency and kinematic effects can be combined in a multiplicative cascade process for the acceleration depending on the kinetic energy and the dissipation rate. On the basis of these observations, we introduce a vectorial stochastic model for the dynamics of a tracer in turbulent flows. This model incorporates a fractional log-normal process for the dissipation rate recently proposed, as well as an additional hypothesis regarding nondiagonal terms in the diffusion tensor which naturally leads to the decomposition between tangential and centripetal acceleration. This model is shown to be in good agreement with direct numerical simulations and presents the essential characteristics of the Lagrangian turbulence highlighted in recent years, namely (i) non-Gaussian acceleration, (ii) scale separation between the norm of the acceleration and its components, (iii) anomalous scaling law for the Lagrangian velocity spectra, and (iv) negative skewness of the increments of the mechanical power, reflecting the temporal irreversibility of the dynamics.

I. INTRODUCTION

With the advances of experimental techniques and the increase in computing power of the last decades, remarkable features of the dynamics of fluid particles in turbulent flows have been discovered. Among other things, the measurement of the probability distribution of the acceleration of these tracers has been shown to be very clearly non-Gaussian with a high frequency of observing very intense events [1–4]. Even for moderate Reynolds numbers, it is relatively common to observe accelerations more than 100 times greater than its standard deviation. In addition, the components of acceleration and its norm present very different correlation times, the ratio of these characteristic

---

*remi.zamansky@imft.fr

times increasing with the Reynolds number [5–7], showing that the dynamics of the tracers is influenced by the full spectrum of turbulence scales. On the one hand, the short-time correlation of the acceleration component is connected to the centripetal forces in intense vorticity filaments [6,8]. On the other hand, the acceleration norm has been shown to be directly correlated with the local dissipation rate of turbulence [9–12], in accordance with Kolmogorov's hypotheses. Nevertheless, various experimental and numerical works have also reported its dependence on local kinetic energy [2,11,13–17], which is generally attributed to nonindependence of the small-scale dynamics from large-scale ones. In this view, the Lagrangian acceleration is essentially given by the local gradients of the velocity, but the latter present correlation with the kinetic energy caused by direct energy transfers between large and small scales in the energy cascade [18]. The absence of proper scale separation explains that the Lagrangian correlation functions present power laws with anomalous exponents which can be described by the multifractal formalism [19–23] as the signature of intermittency and persistence of viscous effects. To end this list, we mention the asymmetry of the fluctuations of the mechanical power received or given up by a fluid particle reflecting the temporal irreversibility of its dynamics [24–28].

Such complex phenomenology must be attributed to the collective and dissipative effects. Indeed, according to the Navier-Stokes equation, the acceleration of a fluid particle is essentially given by the pressure field which is determined by the motion of all the other particles [29,30]. Moreover, although the Laplacian term in the Navier-Stokes equation is of order Re^{-1} smaller than the pressure gradient term, the viscosity cannot be neglected. Indeed, as a small force integrated over a long period could be significant, the viscosity insidiously affects the fluid tracer velocity. Which in turn influences the particle acceleration through modification of the pressure gradient and local interactions are intrinsically inseparable from the nonlocal ones. This is manifested by the persistence of the Reynolds number effect on the acceleration statistics, even for very large Reynolds numbers. Such a scenario is supported by Refs. [31–33] who showed that adding noise to an inviscid Lagrangian flow leads to irreversibility of the dynamics.

Following the Kolmogorov first hypothesis [34,35] stating that locally homogenous turbulent flows are universal, it should be possible, in principle, to propose a stochastic model that reproduces the dynamics of a single fluid particle by effectively accounting for the interactions with all the other fluid particles. Let us note that the Kolmogorov first hypothesis received some support from recent studies [36–38]. To propose such a stochastic model, our main assumption in this paper is to write the increments of the acceleration vector of a fluid particle as $da_i = M_i dt + D_{ij} dW_j$. Both M and D depend on the particle acceleration a and velocity u. The latter is simply given by the kinematic relation of a fluid particle $u_i = \int a_i dt$. It is indeed a necessary condition that a depends on u to present a restoring effect that can counteract the diffusion in velocity space and have statistically stationary dynamics of the fluid particle. We will propose closed expressions for M and D from basic consideration using as a starting point the acceleration statistics conditioned on both the local values of the dissipation rate and the kinetic energy observed from direct numerical simulations (DNS) and presented as well in this paper. It will be shown that introducing a "maximal winding hypothesis" associated to a nondiagonal diffusion tensor, this simple stochastic model reproduces all the statistical feature of the Lagrangian dynamics presented above without any adjustable parameter.

Let us first review some previous works on the stochastic modeling for the Lagrangian dynamics (see also Ref. [13]). Among the pioneering works, Sawford [39] proposed a scalar Gaussian model for the acceleration presenting a feedback term proportional to the velocity. Pope and Chen [40] devised a Langevin like equation for the velocity coupled with a log-normal model for the dissipation through the introduction of conditional statistics. Similarly, Refs. [41–43] proposed an extension of the Sawford model leading to a non-Gaussian scalar model for the acceleration. This work was further refined by Ref. [44] who also advanced a non-Gaussian scalar model for the dynamics by prescribing an ad hoc shape of the conditional acceleration statistics with the dissipation along with a linear dependence on the velocity. The model introduced in Ref. [45] describes increments of the derivative of acceleration in a so-called third-order model to better account for the Reynolds number dependence on the acceleration statistics. Recently, Ref. [46] proposed generalization to an

infinite number of layers leading to smooth 1D trajectory along with a multifractal correction to account for intermittency, as introduced in Refs. [47–49]. An acceleration vector model has been proposed in Ref. [50] by imposing an empirical correlation between velocity and acceleration, with additive noise leading to Gaussian statistics for the acceleration. Likewise, Ref. [51] presented a 3D Gaussian model, with linear dependence on the velocity as well as an extension to nonhomogenous flows. To account for intermittency effect, in Refs. [52–57] the 3D acceleration vector is given by the product of two independent stochastic processes, one for the acceleration norm the other for its orientation. In these models the velocity feedback on the dynamics is realized by a coupling with a large eddy simulation framework. To summarize, to our knowledge, a 3D vectorial model for the tracer dynamics that is autonomous and reproducing the essential features of Lagrangian turbulence (irreversibility, non-Gausianty, multifractality) has not yet been proposed.

The essential building block of previously cited models is the conditional acceleration statistics. Previous studies have focused on conditional statistics with either the velocity or the dissipation rate separately. From the extensive analysis of Ref. [12], one can conclude that the acceleration variance conditioned on the dissipation rate ε presents a power-law behavior for large values of ε with a Reynolds number dependent exponent reflecting that the small-scale dynamics are not independent of large scales.

Regarding the links between the fluid particle acceleration and their velocity, Biferale *et al.* [14] argue that according to the Heisenberg-Yaglom scaling for the acceleration $\langle a^2 \rangle \sim a_\eta^2 = \langle \varepsilon \rangle^{3/2} \nu^{-1/2} = \langle K \rangle^{9/4} L^{-3/2} \nu^{-1/2}$, with ν the kinematic viscosity, $K = 1/2 u_i u_i$ the kinetic energy and L the characteristic size of large structures, one should expect that the variance of the velocity-conditioned acceleration behaves like: $\langle a^2 | K \rangle \propto K^{9/4}$. Then on the basis of the multifractal formalism, they proposed a very close scaling law, $\langle a^2 | K \rangle \sim K^{2.3}$. The proposed relation was observed to be in agreement with DNS for large velocity, typically $|u| > 3\sigma_u$ with $\sigma_u = \sqrt{2/3 \langle K \rangle}$. These events remain very rare since the PDF of the fluid velocity is Gaussian so the range of validity of the power law is, at best, very limited. However, Sawford *et al.* [17] propose that $\langle a_x^2 | u_x \rangle \sim u_x^6$ based on a mechanism involving vorticity tubes. This scaling law which seems compatible with the first measurements of the acceleration conditioned on velocity in Ref. [2], is confirmed neither by the DNS of Ref. [14] nor in a second experimental paper by Crawford *et al.* [16] which gave more credit to the $K^{9/4}$ law. As mentioned above, it has been proposed that the dependence of the acceleration on the velocity arises through the dependence of the dissipation rate on the kinetic energy due to intermittency effect [14]. Additionally, Ref. [18] proposed that the dependence on velocity is a consequence of direct and bidirectional coupling of large and small scales caused by kinematic relations related to nonlocal interactions.

In this paper we study the acceleration statistics conditional on both the kinetic energy and the dissipation rate. To our knowledge such doubly conditional statistics of the acceleration have never been presented. It will be shown that the variance can be expressed as $\langle a^2 | \varepsilon, K \rangle \sim \exp(\alpha K / \langle K \rangle + \gamma \ln \varepsilon / \langle \varepsilon \rangle)$. This result is clearly in contrast with the previously proposed power-law dependence on velocity. It shows that the influence of the large scales through the intermittent distribution of the dissipation rate, which manifests through the Reynolds number dependence of the coefficient γ, is supplemented by an explicit dependence on the local kinetic energy. This direct dependence on the large-scale characteristics is of a kinematic nature as it appears independent of the Reynolds number. The behavior of the doubly conditional acceleration can be interpreted as a consequence of scaling symmetry for the fluid-particle acceleration incorporating both the intermittency and the kinematic effects of the flow structure. We also propose to apply the incomplete similarity framework introduced by Barenblatt to explain the dependence of the statistics of the acceleration conditional to the dissipation rate on the Reynolds number and to account for the intermittency effect. That enables us to provide as well new scaling relations for the unconditional variance in good agreement with the DNS. Eventually the doubly conditional statistic of the acceleration which gives a relation between the force, the energy, and the power will serve as a corner stone to build the stochastic model for the dynamics of a fluid particle mentioned above. Although such a model could

be of interest for practical applications, its construction is relevant to study the specificities of the Lagrangian description of turbulence by linking the cascade picture to the fluid particles dynamics on the basis of the behavior of the conditional statistics obtained by the DNS of the Navier-Stokes equations.

In Sec. II we present the statistic of the acceleration conditioned on the local values of the dissipation rate and kinetic energy obtained from DNS. Then we show that the Reynolds number dependence on the acceleration conditioned on the dissipation rate can be described using the Barenblatt incomplete similarity. We deduce a new relation for the unconditional acceleration variances. To end this section, we show that these new results can be interpreted as a multiplicative cascade for the acceleration with scale dependent kinematic effects. Then in Sec. III we give the derivation of the stochastic model for the single fluid particle dynamics taking as an initial step the doubly conditional acceleration variance, and present the outcome of the model for the Reynolds number up to $\mathrm{Re}_\lambda = 9000$ along with comparison with DNS results when available.

II. SCALING LAWS OF THE ACCELERATION

A. Methodology

We present in this section results concerning the statistics of the acceleration of a fluid particle. These results have been obtained from five direct numerical simulations (DNS) of isotropic turbulence in a periodic box with Taylor-scale Reynolds numbers of $\mathrm{Re}_\lambda = 50, 90, 150, 230,$ and 380. We used pseudospectral code as detailed in Refs. [57–59]. The DNS was carried with resolutions of $128^3, 256^3, 512^3, 1024^3,$ and 2048^3 with the large-scale forcing proposed by Ref. [60]. For each simulation we have $\eta/\Delta x = 1$ with $\eta = \langle \varepsilon \rangle^{-1/4} \nu^{3/4}$ the Kolmogorov length scale and Δx the grid size. The statistics are computed from 40 3D fields sampled at roughly each large-eddy-turnover time.

We will show statistics of the acceleration conditioned by the dissipation rate and the kinetic energy. Note that in this paper we consider the pseudodissipation $\tilde{\varepsilon} = \nu(\partial_j u_i)^2$, which is the second invariant of the velocity gradient tensor multiply by the viscosity rather than the dissipation $\varepsilon = \frac{1}{2}\nu(\partial_j u_i + \partial_i u_j)^2$. We prefer to show here the statistics of the pseudodissipation to be consistent with the next section of the paper, in which we will use the log-normal distribution hypothesis for the dissipation. Indeed, this property is very well verified for the pseudodissipation whereas it is only approximate for the dissipation [12]. Nevertheless, the statistics presented below have also been computed considering the dissipation, ε, and no significant differences were observed. To lighten the paper, in the sequel, we will drop the tilde in the notation of the pseudodissipation, as well, in the text, we will write dissipation instead of pseudodissipation.

B. Conditional statistics given the dissipation and the kinetic energy

To illustrate the relationships between acceleration, energy dissipation and kinetic energy, we show in Fig. 1 visualizations of these quantities at the same instant obtained from our DNS. We notice that $\ln a^2/\langle a^2 \rangle$ and $\ln \varepsilon/\langle \varepsilon \rangle$ show a fairly marked correlation although the acceleration appears more diffuse than dissipation. We also notice that to some extent the kinetic energy and the dissipation rate appears correlated. In addition, it seems that some areas of the flow where the kinetic energy is high also correspond to regions of high acceleration magnitude.

Figure 2 presents the variance of the acceleration of a fluid particle conditioned to the local values of the kinetic energy and the dissipation rate: $\langle a^2|\varepsilon, K\rangle$. In Fig. 2 (top), the levels of the logarithm of the conditional variance are shown as a function of K and of ε. We see that the conditional variance of the acceleration depends on these two quantities and that the dependence on K seems somewhat similar to that of $\ln \varepsilon$. In a more quantitative way, we show in Fig. 2 (left) the variance of the acceleration as a function of ε for different values of K. We can see that the shape of the curves remains globally unchanged when K varies and also presents the same shape as the variance conditioned by ε only as also presented in this figure. Essentially, it is observed that the conditional
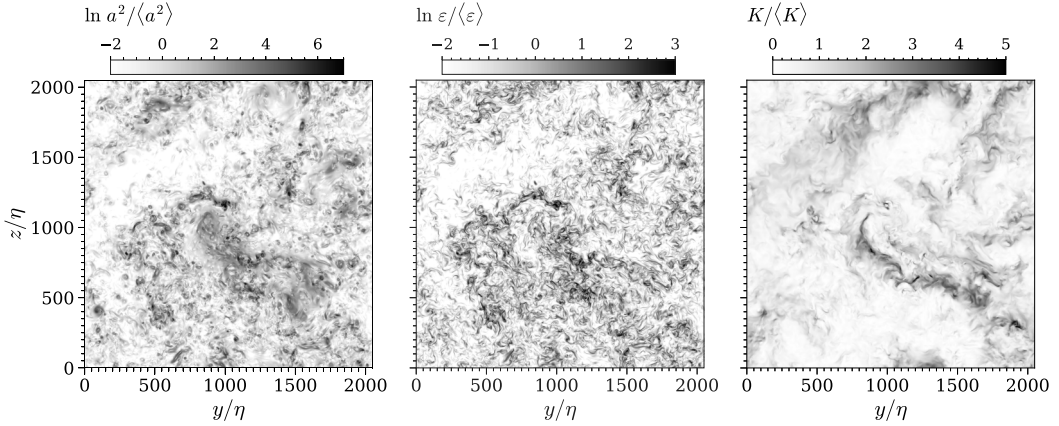
FIG. 1. Visualization of the instantaneous fields of the square of the acceleration, of the dissipation and of the kinetic energy in a cut y-z of the flow by DNS at $\mathrm{Re}_\lambda = 380$. Left: $\ln(a^2/\langle a^2\rangle)$; middle: $\ln(\varepsilon/\langle\varepsilon\rangle)$; right: $K/\langle K\rangle$.
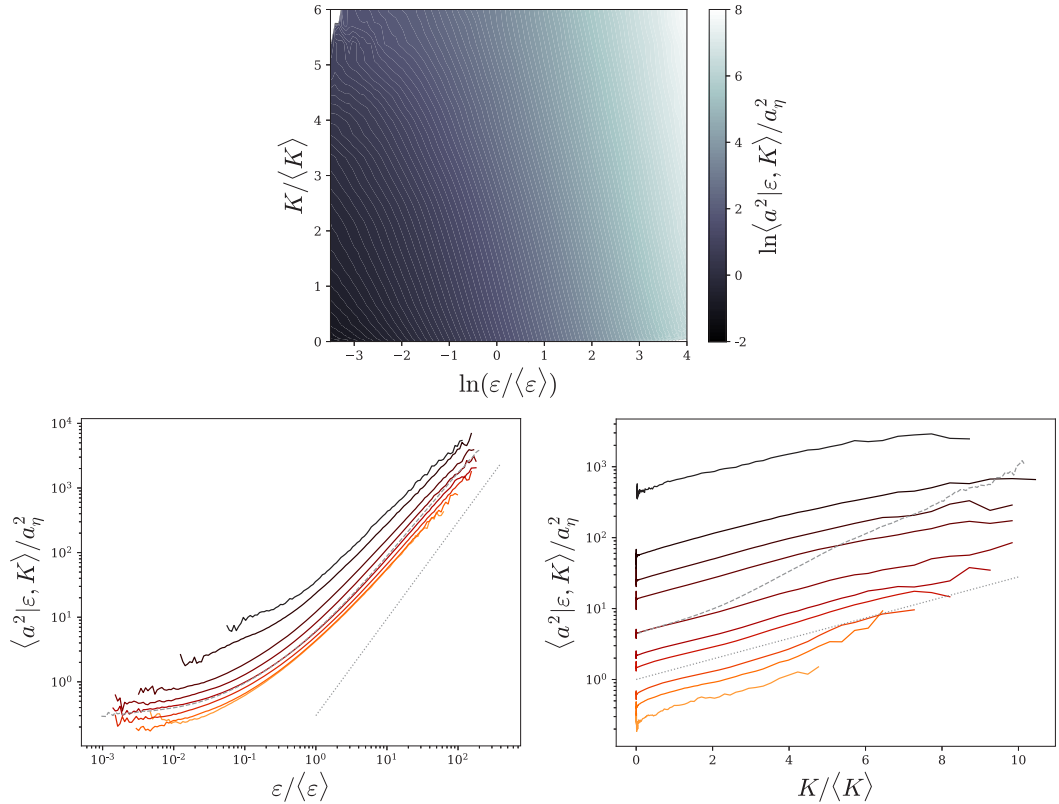

FIG. 2. Variance of acceleration conditioned on the local dissipation rate and kinetic energy obtained from DNS at $\mathrm{Re}_\lambda = 380$. (Top) Map of $\ln\langle a^2|\varepsilon, K\rangle/a_\eta^2$ versus $\ln\varepsilon/\langle\varepsilon\rangle$ and $K/\langle K\rangle$. (Left) Plot, in logarithmic scales, of $\langle a^2|\varepsilon, K\rangle/a_\eta^2$ against $\varepsilon/\langle\varepsilon\rangle$ for $K/\langle K\rangle = 0.025, 0.1, 0.5, 1, 2, 3, 5, 6.5 \pm 30\%$ from orange to black. Comparison with $\langle a^2|\varepsilon\rangle/a_\eta^2$ in gray dashed line and with the power law $(\varepsilon/\langle\varepsilon\rangle)^{3/2}$ in gray dotted line. (Right) Plot, in semilogarithmic scales, of $\langle a^2|\varepsilon, K\rangle/a_\eta^2$ against $K/\langle K\rangle$ for $\varepsilon/\langle\varepsilon\rangle = 0.01, 0.05, 0.1, 0.3, 0.5, 1, 3, 5, 10, 50 \pm 30\%$ from orange to black. Comparison with $\langle a^2|K\rangle/a_\eta^2$ in gray dashed line and with $\exp(\alpha K/\langle K\rangle)$ with $\alpha = 1/3$ in gray dotted line.

variance presents power-law behavior for $\varepsilon \gg \langle \varepsilon \rangle$ with an exponent close to 3/2 and a prefactor depending on K. As discussed in more details below, we observe a slight deviation of the scaling law compared to the acceleration conditioned only by the dissipation.

Figure 2 (right) shows the variance of the acceleration as a function of K for different values of ε. As expected, we find that the variance of the acceleration increases with K. We clearly notice an exponential growth of the variance over the whole range of K with a growth rate α which appears independent of ε:

$$\langle a^2 | \varepsilon, K \rangle = c_\varepsilon a_\eta^2 \exp(\alpha K / \langle K \rangle), \tag{1}$$

with $a_\eta^2 = \langle \varepsilon \rangle^{3/2} \nu^{-1/2} = \langle \varepsilon \rangle / \tau_\eta$ the so-called Kolmogorov acceleration and the prefactor c_ε depending on ε. From our DNS it appears that $\alpha \approx 1/3$ for all the Reynolds numbers considered here. We also find the same value of α from the database of Refs. [61,62] obtained for $\mathrm{Re}_\lambda = 400$ suggesting that the value of α is independent of the Reynolds number.

This exponential behavior contrasts with the references mentioned in the introduction in which power-law behavior for the variance conditioned on K solely had been proposed. Nevertheless, we can notice that exponential growth does not seem to disagree with the data presented in these references. Interestingly, this relationship only depends on a characteristic velocity (not a time and a length scale separately). The absence of characteristic time is attributed to the scale separation between large structures and small ones (the large structures of the flows appear as quasi stationary and infinite to the smallest ones such that only their relative velocity matters). The independence of the coefficient α on the Reynolds number tends to confirm that the velocity scale used for the nondimensionalization of the argument of the exponential is appropriate.

In Appendix A we propose to estimate the factor c_ε as

$$c_\varepsilon \approx A \langle a^2 | \varepsilon \rangle / a_\eta^2, \tag{2}$$

where $A = (1 - \frac{2}{3}\alpha)^{3/2}$, which is equal to $A = 7\sqrt{7}/27 \approx 0.686$, for $\alpha = 1/3$, neglecting a small logarithmic dependence on $\varepsilon / \langle \varepsilon \rangle$.

Consequently, for large Reynolds numbers, the doubly conditioned variance of the fluid-particle acceleration is expressed as

$$\langle a^2 | \varepsilon, K \rangle = A \langle a^2 | \varepsilon \rangle \exp(\alpha K / \langle K \rangle). \tag{3}$$

This relation is confirmed in Fig. 3 which presents the conditional variance of the acceleration normalized by $A a_\eta^2 \exp(\alpha K / \langle K \rangle)$ as a function of ε for different values of K as well as normalized by $A \langle a^2 | \varepsilon \rangle = \langle a^2 | \varepsilon, K = 0 \rangle$ as a function of K for different values of ε. It can be seen that a fairly good overlap of the various curves is obtained, confirming the self-preserving character of the acceleration conditioned on both the kinetic energy and the dissipation rate. We see in this relation an explicit effect of the local kinetic energy on the acceleration. Since the argument of the exponential depends on $K / \langle K \rangle$ not on a local Reynolds number, it suggests pure kinematic effects for the acceleration which is likely associated to the divergence free constrain and the nonlocality of the pressure gradient. There is also indirect effect through the dependence of the dissipation rate on the large-scale structures. The later is manifested as Reynolds number dependence of the conditional acceleration on the dissipation rate solely. This intermittency effect is analyzed further in the next section. We postpone to Sec. II E further comments on the behavior of the doubly conditioned variance.

C. Similarity of the conditional statistics given the dissipation

We propose now to focus with more details on the scaling law of the acceleration variance conditioned on the dissipation rate only, $\langle a^2 | \varepsilon \rangle$. For that we consider the DNS data from Yeung *et al.* [12], along with our DNS data. Figure 4 (left) presents the conditional acceleration variance for Reynolds numbers in the range $\mathrm{Re}_\lambda = 40$ to 680. We first notice that for weak values of
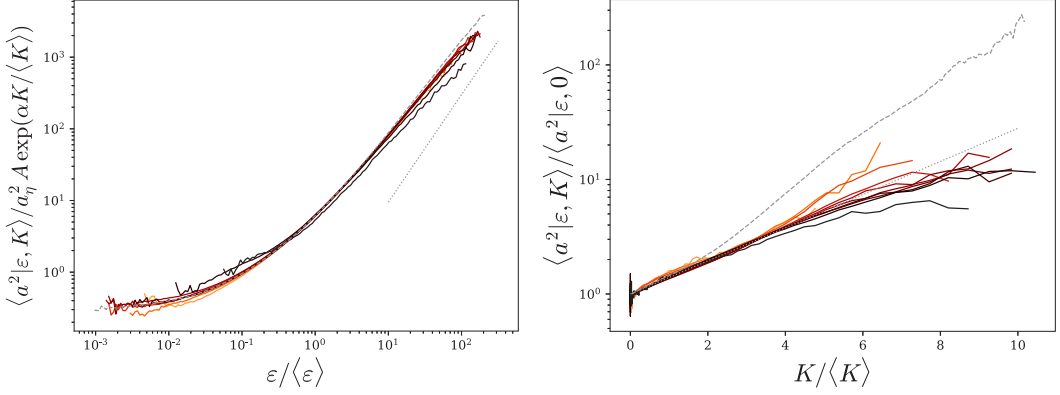
FIG. 3. Normalized variance of acceleration conditioned on the local dissipation rate and kinetic energy obtained from DNS at $\mathrm{Re}_\lambda = 380$. (Left) Plot of $\langle a^2|\varepsilon, K\rangle/Aa_\eta^2 \exp(\alpha K/\langle K\rangle)$ against $\varepsilon/\langle\varepsilon\rangle$ for various values of K. Comparison with $\langle a^2|\varepsilon\rangle/a_\eta^2$ in gray dashed line and with the power law $(\varepsilon/\langle\varepsilon\rangle)^{3/2}$ in gray dotted line. (Right) Plot of $\langle a^2|\varepsilon, K\rangle/\langle a^2|\varepsilon, K = 0\rangle$ against $K/\langle K\rangle$ for various values of $\varepsilon/\langle\varepsilon\rangle$. Comparison with $\langle a^2|K\rangle/a_\eta^2$ in gray dashed line and with $\exp(\alpha K/\langle K\rangle)$ with $\alpha = 1/3$ in gray dotted line The ranges for the fixed values of K and ε for both plots are the same as in Fig. 2.

the dissipation rate ($\varepsilon \ll \langle\varepsilon\rangle$) the value of the conditional acceleration variance tends towards an asymptotic value, which depends on the Reynolds number. The saturation of the conditional acceleration shows that the local acceleration is not only determined by the microstructure of the flow, and that it presents somehow effects of the large structures of the flow which dominates in low dissipative regions. We denote by a_0^2 the asymptotic value of the conditional variance:

$$a_0^2 = \lim_{\varepsilon \to 0}\langle a^2|\varepsilon\rangle. \tag{4}$$
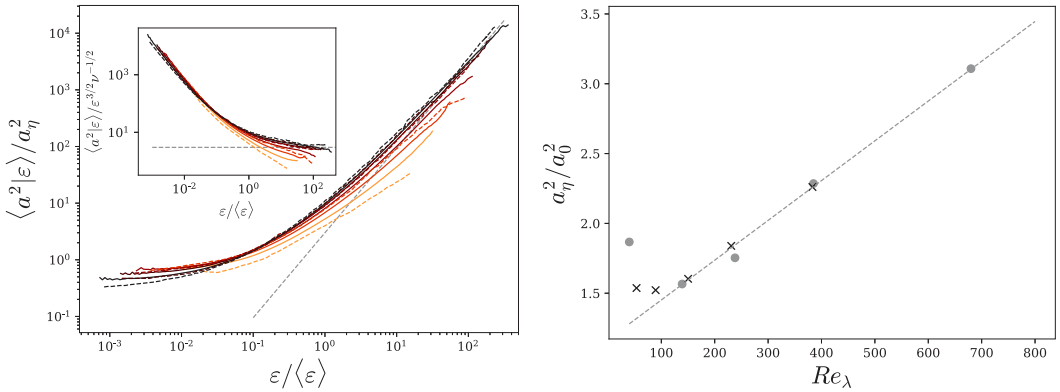

FIG. 4. (Left) Acceleration variance conditioned on the local dissipation rate normalized by the Kolmogorov acceleration $\langle a^2|\varepsilon\rangle/a_\eta^2$. The continuous line are for our DNS for $\mathrm{Re}_\lambda = 50, 90, 150, 230$ and 380 from orange to black; the dashed lines correspond to the DNS of Yeung *et al.* [12] for $\mathrm{Re}_\lambda = 40, 139, 238, 385, 680$, from orange to black. Comparison with the power law $(\varepsilon/\langle\varepsilon\rangle)^{3/2}$. Inset conditional acceleration normalized by $\varepsilon^{3/2}\nu^{-1/2}$. (Right) a_η^2/a_0^2 as a function of Re_λ with $a_0^2 = \lim_{\varepsilon \to 0}\langle a_i^2|\varepsilon\rangle$ the acceleration variance in low dissipative regions. Gray dots for the DNS of Yeung *et al.*, black crosses for our DNS. Comparison with the line $0.0028\mathrm{Re}_\lambda + 1.16$ in dashed lines.

Assuming that the acceleration of fluid particles in low dissipative regions is mainly influenced by large scales, we can estimate a_0^2 as $a_0^2 \sim \langle K \rangle / \tau_L^2$ with τ_L the integral timescale of the flow. This leads to the following estimate:

$$a_0^2/a_\eta^2 \sim \tau_\eta/\tau_L \sim \text{Re}_\lambda^{-1}. \tag{5}$$

We test this scaling law for a_0 in Fig. 4 (right) by presenting a_η^2/a_0^2 as a function of Re_λ from the different DNS datasets. We observe a linear growth rate of a_0^2/a_η^2 with $1/\text{Re}_\lambda$.

For large values of ε, we notice in Fig. 4 (left), as already reported in Ref. [12], that the conditional variance presents a power-law behavior with ε. The exponent of this scaling law is seen to evolve continuously with the Reynolds number, and seems to tend asymptotically towards $\varepsilon^{3/2}$. From dimensional analysis we define f as

$$\frac{\langle a^2 | \varepsilon \rangle}{\varepsilon^{3/2} \nu^{-1/2}} = f(\varepsilon/\langle \varepsilon \rangle, \text{Re}_\lambda). \tag{6}$$

In the inset of Fig. 4 (left), it is seen that f seems to admit an asymptotic constant value for $\varepsilon \gg \langle \varepsilon \rangle$ only in the limit of very large Reynolds number. For intermediate Reynolds numbers, f presents power-law behavior with ε for $\varepsilon \gg \langle \varepsilon \rangle$ but with a Reynolds number dependent exponent. This implies an absence of similarity of the flow when the Reynolds number is changed and the persistence of the Reynolds number effect, even for large Reynolds numbers, which highlights an absence of proper scale separation suggesting direct coupling between large and small scales. This is reminiscent of the incomplete similarity framework proposed by Barenblatt [63–65]. Following Barenblatt, we assume that f presents an incomplete similarity in $\varepsilon/\langle \varepsilon \rangle$ and absence of similarity in Re_λ. Accordingly, we write

$$f(\varepsilon/\langle \varepsilon \rangle, \text{Re}_\lambda) = B(\varepsilon/\langle \varepsilon \rangle)^\beta, \tag{7}$$

where the anomalous exponent β, and the prefactor B are both functions of Re_λ. Arguing for a vanishing viscosity principle, it can be assumed that the critical exponent becomes independent of the Reynolds number in the limit of asymptotically large Reynolds number. Finally assuming that the dependence of B and β on the Reynolds number is small, Barenblatt further proposed that they presents inverse logarithmic dependence on Re_λ, which is also in agreement with the log-similarity proposed by Refs. [66,67]. Expending β and B in power of $1/\ln(\text{Re}_\lambda)$ yields, keeping only the leading-order term in Re_λ:

$$\beta = \beta_0 + \beta_1/\ln \text{Re}_\lambda, \tag{8}$$

$$B = B_0 + B_1/\ln \text{Re}_\lambda. \tag{9}$$

To have a finite limit, consistently with the vanishing viscosity principle, we need $\beta_0 = 0$. The remaining constants B_0, B_1, and β_1 are then determined by comparison with the DNS data. From the inset of Fig. 4 (left) we see that both β and B are increasing functions of Re_λ implying that both B_1 and β_1 are negative. In Fig. 5 (left) we assess the relations (7)–(9) by plotting

$$\chi = \frac{1}{\gamma} \ln \left(1/B \langle a^2 | \varepsilon \rangle / a_\eta^2 \right), \tag{10}$$

with

$$\gamma = 3/2 + \beta, \tag{11}$$

against $\ln(\varepsilon/\langle \varepsilon \rangle)$ for various Reynolds numbers. It is observed that with $B_0 = 17.1$, $B_1 = -54.7$, and $\beta_1 = -1$, all the DNS data collapse on the line $\chi = \ln(\varepsilon/\langle \varepsilon \rangle)$ (the bisectrix of the graph) for $\varepsilon \gg \langle \varepsilon \rangle$, validating the scaling relation.

We can go a step further by using the low dissipative limit of the conditional acceleration. For that we introduce $\chi_0 = \lim_{\varepsilon \to 0} \chi = \frac{1}{\gamma} \ln(1/B \, a_0^2/a_\eta^2)$. With this definition, $\chi - \chi_0 = \ln[(\langle a^2 | \varepsilon \rangle / a_0^2)^{1/\gamma}]$
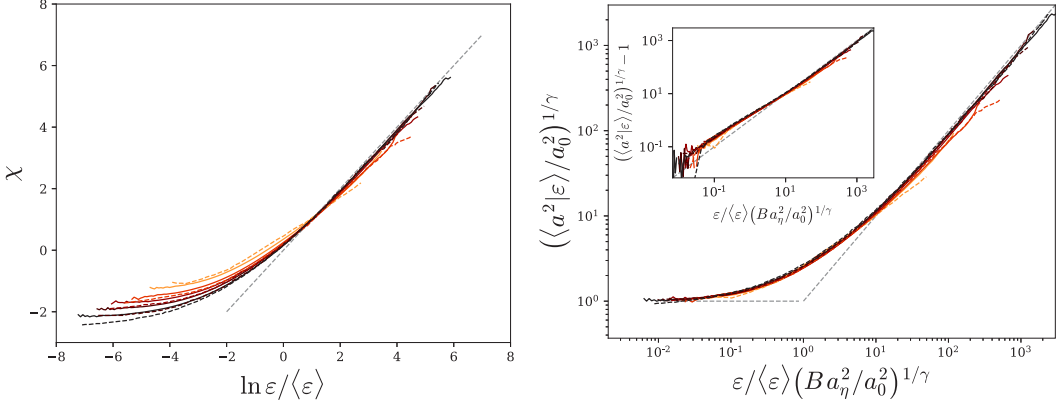
FIG. 5. (Left) Evolution of $\chi = \frac{1}{\gamma} \ln(1/B \langle a^2|\varepsilon \rangle/a_\eta^2)$, with $\gamma = 3/2 + \beta$ versus $\ln \varepsilon/\langle \varepsilon \rangle$ with $B = B_0 + B_1/\ln(\mathrm{Re}_\lambda)$ and $\beta = \beta_1/\ln(\mathrm{Re}_\lambda)$ and $B_0 = 17.1$, $B_1 = -54.7$ and $\beta_1 = -1$, for various Re_λ: continuous line for our DNS at $\mathrm{Re}_\lambda = 50, 90, 150, 230$ and 380 from orange to black; and dashed lines correspond to the DNS of Yeung *et al.* [12] for $\mathrm{Re}_\lambda = 40, 139, 238, 385, 680$, from orange to black. Comparison with the line $\chi = \ln \varepsilon/\langle \varepsilon \rangle$ in gray dashed line. (Right) Evolution of $(\langle a^2|\varepsilon \rangle/a_0^2)^{1/\gamma} = \exp(\chi - \chi_0)$ against $\zeta = \varepsilon/\langle \varepsilon \rangle (B a_\eta^2/a_0^2)^{1/\gamma}$ for the various Reynolds numbers. Inset: plot of $(\langle a^2|\varepsilon \rangle/a_0^2)^{1/\gamma} - 1$ against $\zeta = \varepsilon/\langle \varepsilon \rangle (B a_\eta^2/a_0^2)^{1/\gamma}$.

tends to 0 in the low dissipative regions ($\varepsilon \ll \langle \varepsilon \rangle$). However, for $\varepsilon \gg \langle \varepsilon \rangle$, $\chi - \chi_0$ should be equal to $\chi - \chi_0 = \ln(\varepsilon/\langle \varepsilon \rangle) - \chi_0 = \ln[\varepsilon/\langle \varepsilon \rangle (B a_\eta^2/a_0^2)^{1/\gamma}]$. This is seen in Fig. 5 (right) that presents the evolution of $(\langle a^2|\varepsilon \rangle/a_0^2)^{1/\gamma}$ against

$$\zeta = \varepsilon/\langle \varepsilon \rangle \left(B a_\eta^2/a_0^2 \right)^{1/\gamma} \tag{12}$$

for the various Reynolds numbers considered here.

It is interesting to note that the curves are all overlapping even for intermediate values of ε, suggesting that the conditional acceleration variance can be cast in a self-similar form:

$$\langle a^2|\varepsilon \rangle = a_0^2[\phi(\zeta)]^\gamma, \tag{13}$$

with ϕ a universal function of only one argument $\phi = \phi(\zeta)$ with the asymptotics $\phi(\zeta) = 1$ for $\zeta \ll 1$ and $\phi(\zeta) = \zeta$ for $\zeta \gg 1$. Making a Taylor expansion of ϕ around $\zeta = 0$ and using a matching asymptotic argument, simply yields to

$$\phi(\zeta) = 1 + \zeta. \tag{14}$$

It is seen in the inset of the Fig. 5 (right) that the proposed expression for ϕ gives a good approximation of the data over the whole range of ε and Re_λ. We can indeed observe more than 5 decades of quasilinear growth of $(\langle a^2|\varepsilon \rangle/a_0^2)^{1/\gamma} - 1 = \exp(\chi - \chi_0) - 1$ with ζ.

The nondimensional function f introduced in Eq. (6) can, in consequence, be expressed as

$$f(\varepsilon/\langle \varepsilon \rangle, \mathrm{Re}_\lambda) = B(\varepsilon/\langle \varepsilon \rangle)^\beta \left(1 + \frac{1}{\zeta}\right)^{3/2+\beta}, \tag{15}$$

where the term within the brackets is interpreted as a correction factor for small dissipative regions. Accordingly, we obtain the following expression for the conditional acceleration variance:

$$\langle a^2|\varepsilon \rangle = B a_\eta^2 \left[\left(\frac{1}{B} \frac{a_0^2}{a_\eta^2}\right)^{1/\gamma} + \frac{\varepsilon}{\langle \varepsilon \rangle} \right]^\gamma. \tag{16}$$

As $\gamma = 3/2 + \beta$ and B evolve slowly with Re_λ, their expressions remain speculative and would require a much larger range of Reynolds numbers to be validated.

D. Reynolds number dependence of the unconditional acceleration variance

Assuming the distribution of the dissipation, we can integrate relation (16) to obtain the unconditional variance

$$\langle a^2 \rangle = \int \langle a^2 | \varepsilon \rangle P(\varepsilon) d\varepsilon, \tag{17}$$

and thus propose an alternative formula to the empirical relations proposed in Refs. [12,17,68]. We consider that $\varepsilon/\langle\varepsilon\rangle$ presents a log-normal distribution with parameter $\sigma^2 \approx 3/8 \ln \mathrm{Re}_\lambda/R_c$ with $R_c = 10$ as shown by Ref. [12] from DNS data, consistently with the proposition of Kolmogorov and Oboukhov [35,69]. Notice nevertheless that other expressions for σ^2 have been proposed in the literature reflecting the vanishing viscosity limits [70]. Taking for $\langle a^2 | \varepsilon \rangle$ the expression (16), we perform the integration numerically with the expressions (8) and (9) for β and B with the values of B_0, B_1 and β_1 and the expression of a_0^2/a_η^2 proposed above. The resulting evolution of the acceleration variance with the Reynolds number is presented in Fig. 9. It is seen that the predicted acceleration variance is in very good agreement with the DNS of Ref. [12] and our DNS and is also very close to the relation proposed by Ref. [17] for $\mathrm{Re}_\lambda < 1000$.

The first term within the brackets in Eq. (16) is the footprint of the large-scale structures whose effects is vanishing if the local dissipation rate is larger than $\varepsilon/\langle\varepsilon\rangle \gg (B\, a_\eta^2/a_0^2)^{-1/\gamma}$ and therefore can be neglected when the Reynolds number is large since $a_\eta^2/a_0^2 \sim \mathrm{Re}_\lambda$. Hence, for large Reynolds numbers, Eq. (16) reduces to

$$\langle a^2 | \varepsilon \rangle / a_\eta^2 = B\left(\frac{\varepsilon}{\langle\varepsilon\rangle}\right)^\gamma. \tag{18}$$

With this expression, the acceleration variance is simply estimated from the moments of the log-normal distribution as

$$\frac{\langle a^2 \rangle}{a_\eta^2} = B(\mathrm{Re}_\lambda/R_c)^{9/64 + 3\beta(1+\beta/2)/8}. \tag{19}$$

This expression, also presented in Fig. 9, is shown to converge to the previous estimate as the Reynolds number increases.

In Appendix B, we show that the integral (17) can be expressed from the generalized binomial series expansion. We further obtain the following estimation for the acceleration variance keeping only the first two terms:

$$\frac{\langle a^2 \rangle}{a_\eta^2} = B\left(\frac{\mathrm{Re}_\lambda}{R_c}\right)^{3/16\gamma(\gamma-1)}\left[1 + \gamma\left(\frac{1}{B}\frac{a_0^2}{a_\eta^2}\right)^{1/\gamma}\left(\frac{\mathrm{Re}_\lambda}{R_c}\right)^{-3/8(\gamma-1)}\right]. \tag{20}$$

In Fig. 9, it is seen that this relation almost overlaps with the direct numerical calculation of the variance through Eq. (17). The term within the brackets enables us to measure the contribution from small Reynolds number effects. At $\mathrm{Re}_\lambda \approx 100$, the two estimates (19) and (20) for the variance differ by about 20%, while there is about 8% in difference at $\mathrm{Re}_\lambda \approx 500$. That confirms that the term containing a_0^2 is indeed vanishing at large Reynolds numbers.

The previous estimations of the acceleration variance tend asymptotically to the following power law:

$$\langle a^2 \rangle / a_\eta^2 = 7.62 \mathrm{Re}_\lambda^{9/64}, \tag{21}$$

where we have used Eq. (8) to obtain the value of the prefactor, $R_c^{-9/64} B_0 \exp(3\beta_1/8) \approx 7.62$. This expression is presented as well in Fig. 9, confirming that the convergence toward the power law is very slow, and that Eq. (19) should be considered as an intermediate asymptotic expression for the acceleration variance.

E. Multiplicative cascade for the acceleration

Substituting Eq. (18) into Eq. (3), we can eventually estimate the doubly conditional acceleration variance for large Reynolds numbers as

$$\langle a^2 | \varepsilon, K \rangle / a_\eta^2 = C \exp(\alpha K / \langle K \rangle) \left(\frac{\varepsilon}{\langle \varepsilon \rangle} \right)^\gamma, \tag{22}$$

where $C = AB$, with expressions of A and B determined above.

As mentioned above and apparent in the previous formula, the acceleration depends on the local value of the kinetic energy, along with the local dissipation rate. The acceleration, being mainly due to the pressure gradient, presents a nonlocal behavior. The fact that the acceleration depends on the local kinetic energy but not on a local Reynolds number reflects that its nonlocality is a purely kinematic effect. Further, the exponential dependence on the kinetic energy suggests that the acceleration can respond to structures of all sizes.

To illustrate this point, we discuss a multiplicative cascade model for the acceleration that incorporates effect of the full spectrum of the flow structure. Fluctuations of the locally space-averaged dissipation rate can be modeled by multiplicative cascades [49,71–75]. Such model proposes to express the local dissipation over a volume of size $\ell = L\lambda^n$, with $\lambda < 1$ and L being the large scale of the flow, as the product of n random numbers ξ_i:

$$\varepsilon_\ell = \langle \varepsilon \rangle \prod_{i=1}^{n} \xi_i. \tag{23}$$

Typically, for large n, this yields log-normal distribution of ε_ℓ assuming the ξ_i are independent and identically distributed (and have as well finite variance).

We propose likewise to write the squared acceleration, coarse-grained at scale ℓ, as

$$a_\ell^2 = a_0^2 \prod_{i=1}^{n} \theta_i. \tag{24}$$

The scale-to-scale factor θ_i is given by

$$\theta_i = \exp\left(\frac{\alpha}{\langle K \rangle} \frac{1}{2} v_i^2 \right) (\xi_i)^\gamma = \exp\left(\frac{\alpha}{\langle K \rangle} \frac{1}{2} v_i^2 + \gamma \ln \xi_i \right), \tag{25}$$

where v_i is here the velocity of eddies of size $\ell_i = L\lambda^i$, which is also a fluctuating quantity. The exponential modulation is then interpreted as an entrainment acceleration due to these structures.

With this expression we obtain

$$a_\ell^2 = a_0^2 \exp\left(\frac{\alpha}{\langle K \rangle} \sum_{i=1}^{n} \frac{1}{2} v_i^2 + \gamma \sum_{i=1}^{n} \ln \xi_i \right). \tag{26}$$

Setting $n = \ln(\eta/L)/\ln(\lambda) \sim \ln \mathrm{Re}_\lambda$, η being the Kolmogorov length scale, we have $K = \sum_{i=1}^{n} \frac{1}{2} v_i^2$ due to the additive nature of the kinetic energy. Thereby using Eq. (23), we obtain back Eq. (22) by taking the conditional average of Eq. (26). The order of magnitude of the eddy velocities can be estimated from the Kolmogorov relation, $(\varepsilon_\ell \ell)^{1/3}$, showing that the sum is *a priori* dominated by the large scales but, however, because of the intermittent behavior of ε_ℓ, it may well happen that the the inertial-scale structures can be dynamically important.

Note that in this multiplicative model, we have transposed the statistical relation (22) to an instantaneous version. Such idealization, find support in the invariance of the conditional PDF, which is shown in Appendix C. An other important point to mention, is that although we assume that the local acceleration depends both on K and ε it is not assumed that those two variables are independent.

The dissipation presents large fluctuations leading to very important accelerations and, even if the acceleration orientation is changing rapidly, it can cause a local increase of the velocity. When the kinetic energy becomes significantly larger than its averaged value, then the modulation of the acceleration by the exponential term becomes preponderant, thus offering a feedback mechanism allowing the obtention of the normal fluctuations of the velocity. This dynamic scenario appears consistent with the recent DNS analysis of Ref. [76] showing that the fluid-particles can undergo energy gains in intense dissipative regions and is developed in the next section.

III. STOCHASTIC MODELING OF THE FLUID-PARTICLE DYNAMICS

A. Model formulation

The foregoing multiplicative model suggests that the acceleration norm can be determined from the local kinetic energy and dissipation rate. The relation (22) is pointwise and so it applies equally well to both Lagrangian and Eulerian descriptions. However, in the Lagrangian framework, the kinematic relation between velocity and acceleration allows proposing a model for the acceleration depending only on the local dissipation rate. The evolution of the later along the particle path is to be obtained from a stochastic process. For the derivation of this model, we will rely on the relation (22), in which the contribution from low dissipative events are neglected:

$$a^2 = f(K, \varepsilon) = a_\eta^2 C \left(\frac{\varepsilon}{\langle \varepsilon \rangle} \right)^\gamma \exp \left(\alpha \frac{K}{\langle K \rangle} \right). \tag{27}$$

We express the increments of a^2 as a second order Taylor expansion in K and ε,

$$da^2 = a^2 \left(\alpha \frac{dK}{\langle K \rangle} + \gamma \frac{d\varepsilon}{\varepsilon} + \frac{\alpha^2}{2} \frac{dK^2}{\langle K \rangle^2} + \frac{\gamma(\gamma - 1)}{2} \frac{d\varepsilon^2}{\varepsilon^2} + \gamma \alpha \frac{dK}{\langle K \rangle} \frac{d\varepsilon}{\varepsilon} \right). \tag{28}$$

We consider ε as stochastic variable reflecting the very large number of degrees of freedom that control it. In a fairly general way, we consider that the dissipation ε follows a multiplicative stochastic process:

$$d\varepsilon = \varepsilon \Pi dt + \varepsilon \Sigma dW, \tag{29}$$

where dW are the increments of the Wiener process ($\langle dW \rangle = 0$; $\langle dW^2 \rangle = dt$). We specify the terms Π and Σ below. Substituting Eq. (29) into Eq. (28) one obtains, following the Ito calculus, at first order in dt:

$$da^2 = a^2 \left[\frac{\alpha}{\langle K \rangle} P + \gamma \Pi + \frac{\gamma(\gamma - 1)}{2} \Sigma^2 \right] dt + \gamma a^2 \Sigma dW. \tag{30}$$

We used the identity $dK = u_i du_i = u_i a_i dt = P dt$, where P is the mechanical power per unit of mass exchanged by the fluid particle. Even if Π and Σ are given, Eq. (30) is not closed, as it remains to estimate $P = a_i u_i$, which requires the knowledge of a_i and u_i.

As mentioned in the Introduction, we introduce a vectorial stochastic model for the dynamics of a fluid particle. We are looking for a stochastic process of the form:

$$du_i = a_i dt, \tag{31}$$

$$da_i = M_i dt + D_{ij} dW_j, \tag{32}$$

where dW_j are the increments of the jth component of a tridimensional Wiener process ($\langle dW_j \rangle = 0$; $\langle dW_i dW_j \rangle = dt \delta_{ij}$). A priori, the vector M and the tensor D depend on the vectors a and $u = \int a dt$. Indeed, M must depend on u to allow the particle velocity to reach a statistically steady state.

Now, we propose expressions for M_i and D_{ij}. For this, we want to impose, on the one hand, that the model is isotropic ($\langle a_i a_j \rangle = 0$ for $i \neq j$) and, on the other hand, that its norm $a^2 = a_i a_i$ is

compatible with Eq. (30). We therefore write the stochastic equation for $a_{ij}^2 = a_i a_j$ derived from Eq. (32), thanks to the Ito formula:

$$
\begin{aligned}
da_{ij}^2 &= a_j da_i + a_i da_j + da_i da_j \\
&= (M_i a_j + M_j a_i + D_{ik} D_{jk}) dt + (a_j D_{ik} + a_i D_{jk}) dW_k.
\end{aligned}
\tag{33}
$$

For the square of the norm $a^2 = a_i a_i$, we have

$$
da^2 = (2a_i M_i + D_{ij} D_{ij}) dt + 2a_i D_{ij} dW_j.
\tag{34}
$$

We then proceed by identification between Eqs. (34) and (30), in a similar way as Refs. [77,78], by identifying first the square of the diffusion term and then the drift term.

1. Identification of the diffusion term and the maximum winding hypothesis

Quite generally, we can decompose the diffusion tensor into

$$
D_{ij} = c_1 \delta_{ij} + S_{ij} + \Omega_{ij},
\tag{35}
$$

where S_{ij} is a zero-trace symmetric tensor and Ω_{ij} is an antisymmetric tensor. The latter can be written as $\Omega_{ij} = \epsilon_{ijk} \omega_k$ with ϵ_{ijk} the Levi-Civita permutation symbol and ω_k a pseudovector. S_{ij} must be zero to guarantee the statistical isotropy of the acceleration. But Ω_{ij} can be different from 0. Indeed, the experimental results of Ref. [3] and numerical results of Ref. [7] have shown that the acceleration presents a scale separation between the evolution of the components and its norm, and that this separation can be modeled using processes for the acceleration norm and its orientation vector [54,55,79]. A stochastic model for orientation can be formulated as a diffusion process with a rotational part in the diffusion tensor [54,80]. Since the model for the dynamics (31) and (32) involves only two vectors, a and u, we propose to form the pseudovector ω from these two vectors to get a closed model: $\omega_k = c_2 \epsilon_{klm} a_l u_m$. The model remains statistically isotropic and the chirality of the flow is not broken either since the odd moments of dW_j are zero (Gaussian with zero mean). In other words, the sign of c_2 does not matters. We then have

$$
D_{ij} = c_1 \delta_{ij} + c_2 (a_i u_j - a_j u_i).
\tag{36}
$$

It is to be noted that c_1 and c_2 are not constant.

By identifying the square of the diffusion term between Eqs. (30) and (34) we find

$$
\gamma^2 (a^2)^2 \Sigma^2 = 4 a_i a_j D_{ik} D_{jk}.
\tag{37}
$$

Expanding it by using expression (36), we find

$$
\gamma^2 (a^2)^2 \Sigma^2 = 4a^2 \big[c_1^2 + c_2^2 (2a^2 K - P^2) \big],
\tag{38}
$$

which gives for c_1

$$
c_1^2 = \frac{\gamma^2}{4} a^2 \Sigma^2 - c_2^2 (2a^2 K - P^2) = a^2 \left[\frac{\gamma^2}{4} \Sigma^2 - 2 c_2^2 K \left(1 - \frac{a_T^2}{a^2} \right) \right],
\tag{39}
$$

where we have introduced the tangential acceleration a_T, as the projection of the acceleration vector in the direction of the velocity vector: $a_T = a_i u_i / \sqrt{u^2} = P / \sqrt{2K}$. Equation (39) imposes a constraint on c_2 to guarantee the positivity of c_1^2:

$$
c_2^2 2K \leqslant \frac{\gamma^2}{4} \Sigma^2,
\tag{40}
$$

since $0 \geqslant 1 - \frac{a_T^2}{a^2} \geqslant 1$. So, to guarantee the positivity of c_1^2 whatever K, c_2^2 must be proportional to $1/K$. Introducing a parameter c_R as $c_2^2 = \frac{\gamma^2}{4} \Sigma^2 \frac{c_R^2}{2K}$, with the constraint $c_R^2 \leqslant 1$, we obtain

$$
c_1^2 = \frac{\gamma^2}{4} \Sigma^2 \big(a^2 (1 - c_R^2) + c_R^2 a_T^2 \big).
\tag{41}
$$

Subsequently, we only consider the limit $c_R = 1$ that corresponds to the maximum rotational part of the diffusion tensor. We will discuss this choice in more detail below in Sec. III C, when presenting the results.

Finally, from Eq. (36) and the expressions of c_1 and c_2, we write the components of the diffusion tensor as

$$D_{ij} = \sqrt{\frac{\gamma^2}{4}\Sigma^2}\left[\sqrt{a_T^2}\delta_{ij} + \sqrt{a_N^2}\epsilon_{ijk}b_k\right], \tag{42}$$

where we introduced the normal component a_N of the acceleration $a_N^2 = a^2 - a_T^2$, and the bi-normal unit vector[1] $b_k = \epsilon_{klm}u_l a_m/|\epsilon_{hij}u_i a_j|$.

Note that b_k, a_T, and a_N are not well defined when $K = 0$. However, c_2 must vanish when $u = 0$, and we can therefore consider that $c_R = 0$ in that case.

2. Determination of the drift term

Identifying the drift term between Eqs. (34) and (30), we get

$$2a_i M_i + D_{ij}D_{ij} = a^2\left(\frac{\alpha}{\langle K\rangle}P + \gamma\Pi + \frac{\gamma(\gamma-1)}{2}\Sigma^2\right). \tag{43}$$

From Eq. (42) the term $D_{ij}D_{ij}$ is computed as[2]

$$D_{ij}D_{ij} = \frac{\gamma^2}{4}\Sigma^2\left(2a^2 + a_T^2\right). \tag{44}$$

We then have

$$a_i M_i = a^2\left(\frac{\alpha}{2\langle K\rangle}P + \frac{\gamma}{2}\Pi - \frac{\gamma}{4}\Sigma^2\right) - a_T^2\frac{\gamma^2}{8}\Sigma^2. \tag{45}$$

To go further we must now specify the terms Π and Σ used for the stochastic process for ε. Various models for the dissipation have been proposed. Pope and Chen [40] proposed a simple model based on the exponential of an Orstein-Uhlenbeck process (see Appendix D 2). Here, we rely on the model proposed in Refs. [78,81]. This non-Markovian log-normal model presents a logarithmic decrease in the correlation of ε which is consistent with the idea of a turbulent cascade and a multiplicative process (see Appendix D 1), unlike the Pope and Chen model which gives an exponential decrease, see also the discussion in Ref. [82]. As presented in Appendix D 2, the drift and diffusion terms are written, respectively, as

$$\Pi = \frac{1}{\tau_\varepsilon}\left(-\ln\frac{\varepsilon}{\langle\varepsilon\rangle} + \frac{\sigma^2}{2\Lambda^2}\left(\frac{\tau_\varepsilon}{\tau_c} - \Lambda^2\right) + \frac{\sigma}{\Lambda}\hat{\Gamma}\tau_\varepsilon\right) \tag{46}$$

and

$$\Sigma = \sqrt{\frac{\sigma^2}{\Lambda^2\tau_c}}, \tag{47}$$

with σ^2 the variance of the logarithm of ε, τ_ε the correlation time of ε, τ_c the regularization timescale of the process (taken equal to the Kolmogorov dissipative time τ_η), Λ^2 a normalization factor, and

---

[1]To obtain this relation we notice that $a_i u_j - a_j u_i = \epsilon_{ijk}\epsilon_{klm}a_l u_m$ and that the vector b_k is the unit vector collinear to $\epsilon_{klm}a_l u_m$: $b_k = \epsilon_{klm}a_l u_m/|\epsilon_{hij}a_i u_j|$. By expanding the norm, we have $(\epsilon_{hij}a_i u_j)^2 = 2a^2 K - P^2$. We therefore write $\epsilon_{klm}a_l u_m = b_k\sqrt{2a^2 K - P^2} = b_k\sqrt{2K}\sqrt{a^2 - a_T^2} = b_k\sqrt{2K}\sqrt{a_N^2}$.

[2]$D_{ij}D_{ij} = \frac{\gamma^2}{4}(a_T^2\underbrace{\delta_{ij}\delta_{ij}}_{3} + a_N^2\underbrace{\epsilon_{ijk}b_k\epsilon_{ijl}b_l}_{2\delta_{kl}b_k b_l})$, $\delta_{kl}b_k b_l = 1$ since b is a unit vector and with $a^2 = a_T^2 + a_N^2$, we obtain

the result.

$\hat{\Gamma}$ the convolution of the Wiener increments with a temporal kernel, ensuring the non-Markovian property of the process. In the process for ε proposed by Refs. [78,81], the latter corresponds to a fractional Gaussian noise with 0 Hurst exponent [83] regularized at scale τ_c. The expression of the convolution kernel proposed by Refs. [78,81], and recalled in the Appendix D 2, applies to a scalar noise since the dissipation rate is a scalar, whereas the acceleration model involves a vectorial noise. Therefore, the kernel in $\hat{\Gamma}$ includes a projection to apply to the vectorial Wiener increments:

$$\hat{\Gamma} = -\frac{1}{2} \int_{-\infty}^{t} \frac{1}{(t - s + \tau_c)^{3/2}} \mathcal{P}_j dW_j(s). \tag{48}$$

By proceeding in a similar way as Ref. [78], the projection operator is obtained by identification between the diffusion terms of Eqs. (30) and (34):

$$\mathcal{P}_j = \frac{2a_i D_{ij}}{\gamma a^2 \Sigma} = \frac{\sqrt{a_T^2} - a_T}{a^2} a_j + e_j, \tag{49}$$

where we have used the relation recall in footnote 1 and where e_j is the unit vector tangent to the trajectory, $e_i = u_i/\sqrt{2K}$. It is interesting to remark that the rotational part of the diffusion tensor induces an asymmetry of the projector between positive and negative power exchange (recall that $P = \sqrt{2K}a_T$). Indeed, for $P \geqslant 0$, $\mathcal{P}_j = e_j$ while for $P < 0$ one has $\mathcal{P}_j = (1 - 2p^2)e_j - 2p\sqrt{1 - p^2}b_j$ with $p = P/\sqrt{2Ka^2}$. In both cases, as it can be readily checked, $\mathcal{P}$ is a unit vector.

Substituting expressions (46) and (47) for Π and Σ in Eq. (45) we have

$$a_i M_i = a^2 \left[\frac{\alpha}{2\langle K \rangle} P - \frac{\gamma}{2\tau_\varepsilon} \left(\ln \frac{\varepsilon}{\langle \varepsilon \rangle} + \frac{1}{2}\sigma^2 - \frac{\sigma}{\Lambda} \hat{\Gamma}\tau_\varepsilon \right) \right] - a_T^2 \frac{\gamma^2}{8} \frac{\sigma^2}{\Lambda^2 \tau_c}. \tag{50}$$

According to Eq. (27), we can write

$$\ln \left(\frac{\varepsilon}{\langle \varepsilon \rangle} \right) = \frac{1}{\gamma} \left(\ln \frac{a^2}{a_\eta^2} - \ln C - \alpha \frac{K}{\langle K \rangle} \right), \tag{51}$$

which gives, once substituted into Eq. (50),

$$a_i M_i = a^2 \left[\frac{\alpha}{2\langle K \rangle} \left(P + \frac{K}{\tau_\varepsilon} \right) - \frac{1}{2\tau_\varepsilon} \left(\underbrace{\ln \left(\frac{a^2}{a_\eta^2} \right) - \ln C + \frac{\gamma}{2}\sigma^2 - \gamma \frac{\sigma}{\Lambda} \hat{\Gamma}\tau_\varepsilon}_{-\hat{\Gamma}_*} \right) \right] - \frac{a_T^2}{\tau_c} \underbrace{\frac{\gamma^2}{8} \frac{\sigma^2}{\Lambda^2}}_{\sigma_*^2}. \tag{52}$$

To simplify the notations, we have introduced $\hat{\Gamma}_* = \gamma \frac{\sigma}{\Lambda} \hat{\Gamma}\tau_\varepsilon + \ln C - \frac{\gamma}{2}\sigma^2$ and $\sigma_*^2 = \frac{\gamma^2}{8} \frac{\sigma^2}{\Lambda^2}$. It is interesting to notice that in Eq. (52) the terms $P + \frac{K}{\tau_\varepsilon} = \frac{dK}{dt} + \frac{K}{\tau_\varepsilon}$ acts as a penalization leading the correlation of the kinetic energy to decay exponentially.

We then propose for M_i an expression compatible with Eq. (52). Proceeding by identification, we have the following relation:

$$M_i = \frac{\alpha}{2\langle K \rangle} \left[\lambda a_i P + (1 - \lambda)a^2 u_i + a_i \frac{K}{\tau_\varepsilon} \right] - a_i \left[\ln \left(\frac{a^2}{a_\eta^2} \right) - \hat{\Gamma}_* \right] \frac{1}{2\tau_\varepsilon} - \frac{\sigma_*^2}{\tau_c} \frac{a_T^2}{a^2} a_i + B_i, \tag{53}$$

where we have introduced the vector B_i, such that $B_i a_i = 0$ as well as the factor λ that both account for the indeterminacy inherent to the inverse projection. By assuming again that there are only two vectors at our disposal, we can take $B_i = \frac{\alpha}{2\langle K \rangle}\lambda'(Pa_i - a^2 u_i)$ by introducing the factor λ'. Note that from the point of view of the projection, the factors λ and λ' are arbitrary in the sense that the scalar product of a_i and Eq. (53) gives Eq. (52) whatever their values. We can nevertheless notice that the

terms involving λ and λ' can be combined, and, by noting $c_u = \lambda + \lambda'$, we get

$$M_i = \frac{\alpha}{2\langle K \rangle}\left[a_i\left(c_u P + \frac{K}{\tau_\varepsilon}\right) - (c_u - 1)a^2 u_i\right] - a_i\left[\ln\left(\frac{a^2}{a_\eta^2}\right) - \hat{\Gamma}_*\right]\frac{1}{2\tau_\varepsilon} - \frac{\sigma_*^2}{\tau_c}\frac{a_T^2}{a^2}a_i. \quad (54)$$

We can notice that the terms of the first line correspond to the coupling with the velocity, those of the second take into account the log-normal character of the dissipation and the last term is due to the rotational part of the diffusion tensor. The diffusion term (42) becomes, by using expression (47),

$$D_{ij} = \sqrt{\frac{2\sigma_*^2}{\tau_c}}\left[\sqrt{a_T^2}\delta_{ij} + \sqrt{a_N^2}\epsilon_{ijk}b_k\right]. \quad (55)$$

We have thus specified our stochastic model for the dynamics of a fluid particle. It is given by Eqs. (31), (32), (54), and (55).

B. Parameters and numerical approach

From a dimensional point of view, to determine the physical parameters of the stochastic model, one must specify time and velocity scales as well as a Reynolds number. This amounts, for example, to imposing the average kinetic energy $\langle K \rangle$, the average dissipation rate $\langle \varepsilon \rangle$ and the viscosity ν. From these physical parameters, we calculate $a_\eta^2 = \langle \varepsilon \rangle^{3/2}\nu^{-1/2}$, $\tau_\eta = \langle \varepsilon \rangle^{-1/2}\nu^{1/2}$. We can also get the Reynolds number based on the Taylor scale $\mathrm{Re}_\lambda = u'\lambda/\nu = 2\sqrt{15}/3\,\langle K \rangle/\sqrt{\langle \varepsilon \rangle \nu}$ with $u' = \sqrt{2\langle K \rangle/3}$ and $\lambda^2 = 15\nu u'^2/\langle \varepsilon \rangle$. We then deduce the Lagrangian integral times scale τ_L as $\tau_L = 0.08\mathrm{Re}_\lambda\tau_\eta$ from the DNS results reported by Refs. [84,85].

The parameter σ^2 is estimated using the relation given by Ref. [12]: $\sigma^2 \approx 3/8\ln\mathrm{Re}_\lambda/R_c$ with $R_c \approx 10$ compatible with the prediction of Kolmogorov and Obhoukov [35,69]. As mentioned in Refs. [35,74], the specific value of R_c is depending on the large scales. Since the influence of the large scales is neglected in our modeling (see Sec. II D), we choose in the following simply $\sigma^2 \approx 3/8\ln\mathrm{Re}_\lambda$. We set as well $\alpha = 1/3$ and $\gamma = 3/2 + \beta$ with $\beta = -1/\ln\mathrm{Re}_\lambda$ in accordance with the results of the DNS presented above. The prefactor C is computed as $C = c_0 A B$ where $A = (1 - \frac{2}{3}\alpha)^{3/2} \approx 0.686$, $B = 17.1$–$54.7/\ln\mathrm{Re}_\lambda$ as determined by DNS. The term c_0 is introduced so that the predicted acceleration variance follows Eq. (19), as one would expect from the construction of the stochastic model, despite the fact that we take $\sigma^2 = 3/8\ln\mathrm{Re}_\lambda$ instead of $\sigma^2 = 3/8\ln\mathrm{Re}_\lambda/R_c$. Consequently, we have $c_0 = (1/\mathrm{Re}_c)^{9/64 + 3\beta/8(1+\beta/2)}$.

For simplicity we have used $\tau_c = \tau_\eta$ and $\tau_\varepsilon = \tau_L$. From τ_ε and τ_c we calculate the value of the normalizing constant Λ as explained in Appendix D 2. Finally, for the parameter c_u, which is the only free parameter of the model, we have determined numerically that with $c_u = 5.22$ the ratio $K/\langle K \rangle$ is 1 on average for all values of the Reynolds number.

The sample paths of this model are obtained by numerical integration of the stochastic differential equation. Numerical integration is made with an explicit Euler scheme by taking a time-step $dt = \tau_{\eta,\min}/100$ with $\tau_{\eta,\min} = \sqrt{\nu/\varepsilon_{\max}}$, an estimation of the minimum dissipative timescale likely to happen during the simulation. This is estimated from the log-normal distribution of the dissipation: $\tau_{\eta,\min} = \tau_\eta \exp(-x\sigma/2 + \sigma^2/4)$, with $x = 6$ by considering that the probability that a random number following the normal distribution reaches a value of 6 standard deviation is sufficiently low [see Eq. (D11)].

For the calculation of the convolution term $\hat{\Gamma}$ appearing in Eq. (54), we propose in Appendix D 3 an efficient algorithm.

A simple Python script presenting the algorithm used to integrate the proposed stochastic model is available in Supplemental Material [86].
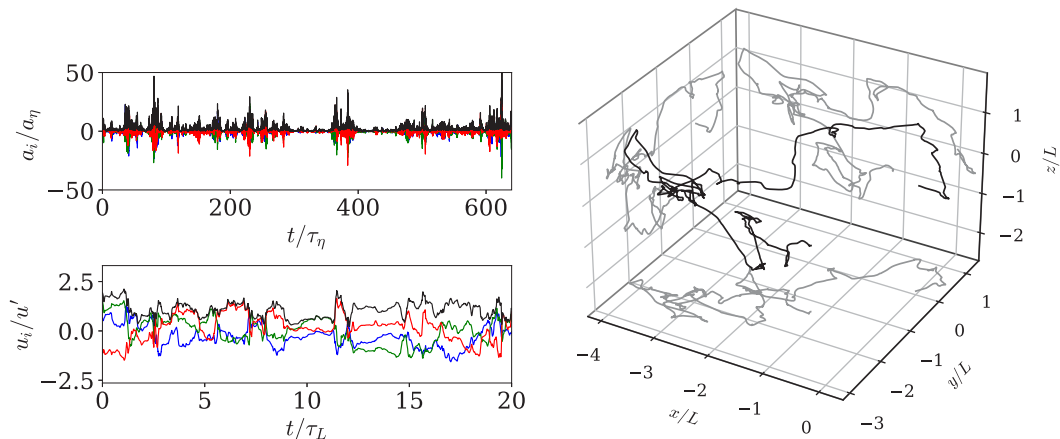
FIG. 6. A realization of the stochastic process for $Re_\lambda = 1100$. Top left: evolution of the acceleration with time a_x, red; a_y, green; a_z, blue; $|a|$, black. Bottom left: evolution of the velocity with time u_x, red; u_y, green; u_z, blue; $|u|$, black. Right: 3D trajectory of a fluid particle for a duration of 100 τ_L.

C. Results

We show in Fig. 6 a realization of this process for $Re_\lambda = 1100$. We see the temporal evolution of the components of acceleration and velocity. There is a very intermittent acceleration with an alternation of periods in which the acceleration of the fluid particle is almost zero with phases of very intense activity. This results in fluid-particle trajectories, obtained by integration of the velocity $x_i = \int u_i(t)dt$, in long quasiballistic periods with typical length of the order of the integral scale $(L \approx \langle K \rangle^{3/2}/\langle \varepsilon \rangle)$ and short term disruptions during which the trajectory rolls up on itself.

We have simulated the stochastic model for 15 different Reynolds numbers between $Re_\lambda = 70$ and 9000. In each case, we have computed 26,000 realizations. The simulations are carried out over a period of $120\tau_L$, over which we exclude an initial transitional regime of $20\tau_L$ for the calculation of the statistics. In all cases, the initial value of the components of acceleration and velocity are sampled from the normal distribution having a standard deviation of $10^{-9}a_\eta$ for the acceleration and $10^{-9}\sqrt{2\langle K \rangle/3}$ for the velocity. We can indeed notice from Eqs. (54) and (55) that, if the acceleration is exactly zero, the stochastic model predicts that the acceleration would remain so. However, it should be noted that this event has a zero probability, and that for arbitrarily small, but nonzero, accelerations, the model presents an evolution towards a nontrivial stationary state. This is illustrated in Fig. 7, which presents the temporal evolution of the variance of the velocity and of the acceleration for $Re_\lambda = 1100$, calculated from all the realizations.

Figure 8 shows the evolution with the Reynolds number of the mean kinetic energy in the stationary state. In this figure, we see that the average kinetic energy is equal, within the statistical convergence, to the value prescribed to the model. We note that the value of the average kinetic energy is directly related to the value of the parameter c_u in Eq. (54) as mentioned above.

Regarding the variance of the acceleration, we expect, by construction of the stochastic model, that the predicted value follows the log-normal relation (19). We observe in Fig. 9 that it is indeed the case, with only slight deviations for the largest Reynolds numbers which are attributed to numerical errors. We recall that the underestimation of the acceleration variance at small Reynolds numbers compared to the DNS or Eq. (20) stems from the fact that the model is based on the relation (22) in which the effect of low dissipative and large-scale structures are neglected (see the discussion in Sec. II C). This simplification enables us to obtain the analytical formulation of the model proposed here.

Figure 10 compares the autocorrelation of the components of the acceleration and of its norm calculated from the stochastic model for $Re_\lambda = 400$ with the calculations from the DNS of
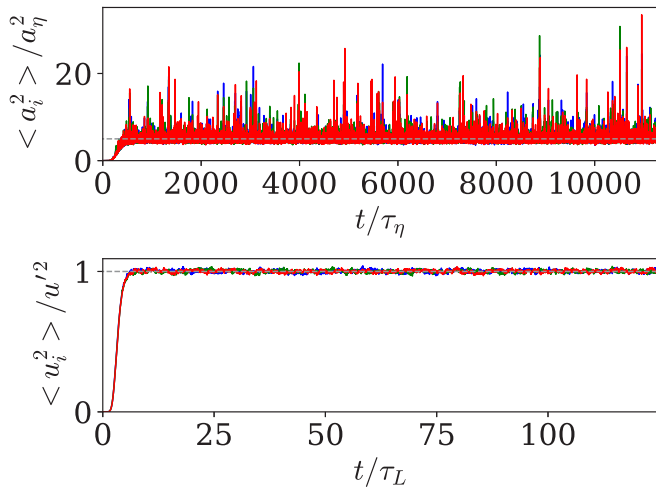
FIG. 7. Evolution of the acceleration and velocity variance with time for the stochastic model at $\mathrm{Re}_\lambda = 1100$ starting from an initial condition for the acceleration and velocity with very small magnitude. Comparison in dashed gray line with the expected values: Eq. (19) for the acceleration and the prescribe value of $u' = \sqrt{2\langle K\rangle/3}$ for the velocity.

Refs. [61,62]. It can be seen that the characteristic times of these two quantities are very different and that it is in good agreement with the DNS. It should be mentioned that the scale separation between the components and the norm results from the rotational part of the diffusion tensor. Indeed, no scale separation is found when c_R is set to zero in Eq. (41) (corresponding then to a diagonal diffusion tensor). We see in Eq. (42) that considering this rotational part, leads to the decomposition of the acceleration into its normal and tangential component. The former is associated with the intense rotation that rapidly changes the acceleration direction, whereas the second is associated with the variation of the kinetic energy of the particle.

Figure 10 also presents the evolution of the autocorrelation coefficient of the velocity components and of the power. It can be seen here also that the agreement with the DNS is relatively good. In
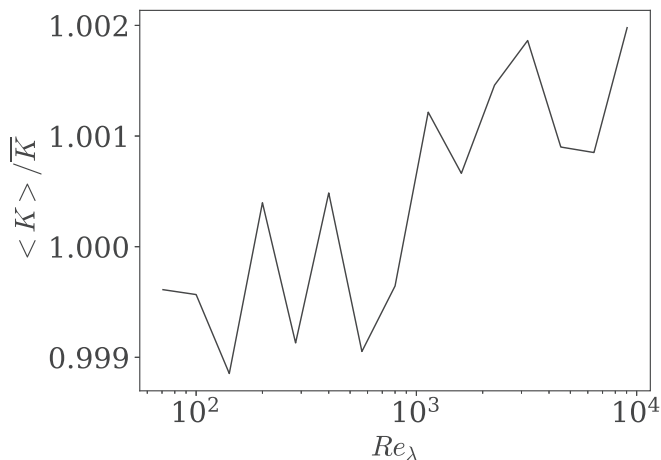

FIG. 8. Evolution with the Reynolds number, in the stationary regime, of the kinetic energy obtained by the stochastic model normalized by the prescribed kinetic energy $\langle K\rangle$.
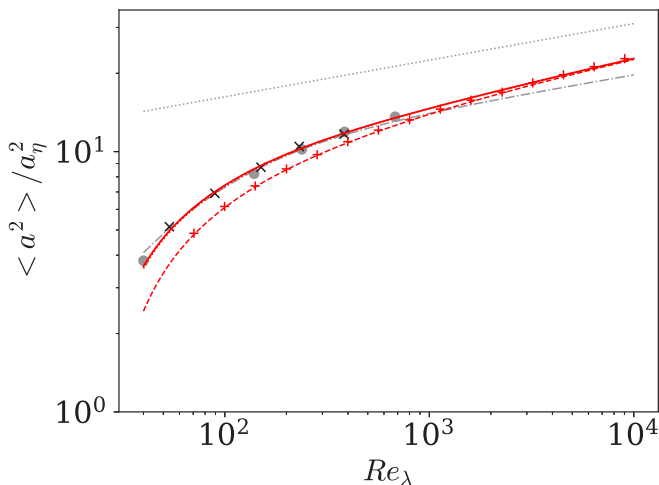
FIG. 9. Evolution with the Reynolds number, in the stationary regime, of the kinetic energy normalized by the prescribed kinetic energy $\langle K \rangle$ (left) and of the acceleration variance normalized by the Kolmogorov acceleration (right). Data from the stochastic model (red plus) and comparison with our DNS data (black crosses) and the DNS data from Ref. [12] (gray dot-dash line), with the relation $3 \times 1.9\mathrm{Re}_\lambda^{0.135}(1 + 85\mathrm{Re}_\lambda^{-1.35})$ from Ref. [17] (gray dash dot line), with the numerical integration of $\langle a^2 \rangle = \int \langle a^2 | \varepsilon \rangle P(\varepsilon) d\varepsilon$ with $\langle a^2 | \varepsilon \rangle$ given by Eq. (16) and $P(\varepsilon)$ log-normal (continuous red line), with its approximation of Eq. (20) (red dotted lines), with the large-Reynolds number limit relation (19) (red dashed line) and with the asymptotic power law (21) (gray dotted lines).

Fig. 10, we also show the evolution of the characteristic correlation times for these four quantities with Reynolds numbers in the range $\mathrm{Re}_\lambda = 70$–9000 as predicted by the stochastic model. The characteristic correlation time for the velocity, the acceleration norm, the acceleration components and the power are $\tau_u = \int \rho_{u_i}(\tau) d\tau$, $\tau_{|a|} = \int \rho_{|a|}(\tau) d\tau$, $\tau_{a_i} = \int |\rho_{a_i}|(\tau) d\tau$ and $\tau_P = \int |\rho_P|(\tau) d\tau$. It can be seen in Fig. 10 that the scales for the norm of the acceleration and for the velocity normalized by τ_L remains quasiconstant with the Reynolds number and that the ratio between the correlation scale for the velocity and τ_L is of order 1. Note that the characteristic time entering the model formulation is τ_ε (the correlation time of the dissipation rate following the path of a fluid particle). For the calculation of the model, we simply set $\tau_\varepsilon = \tau_L$ arguing that the two quantities should be closed. It is therefore interesting to remark that the integral time of the velocity is very close to the prescribe one $\tau_u \approx \tau_L$. Regarding the correlation scales for a component of acceleration and for the power normalized by τ_L, they both present a variation close to $1/\mathrm{Re}_\lambda$, as expected.

We also show in Fig. 10 autocorrelation coefficient of a_i, $(a^2)^{1/2}$, $P = a_i u_i$ and u_i for Reynolds numbers in the range $\mathrm{Re}_\lambda = 70$–9000 obtained from the model. It is seen that, when the time shift is normalized by the corresponding integral timescale, the correlation coefficients of the power and of the acceleration component remains nearly unchanged with the Reynolds number. We observe as well that the shape of the autocorrelation obtained from DNS is well reproduced, although the decay predicted by the model is too fast at very short time lag. This is attributed to the fact that the dissipative region is only taken into account in the model via the cutoff $\tau_c = \tau_\eta$ of the kernel $\hat{\Gamma}$. We observe that the correlation for the acceleration norm presents a logarithmic decrease, reflecting the absence of characteristic time for its evolution. As expected, the correlation norm exhibits a lower slope as the Reynolds number increases. This is directly attributed to the use of the non-Markovian process of Ref. [81] for the dissipation rate, which proposes a logarithmic evolution of the autocorrelation in agreement with the underlying model of the turbulent energy cascade as discussed in Appendix D.
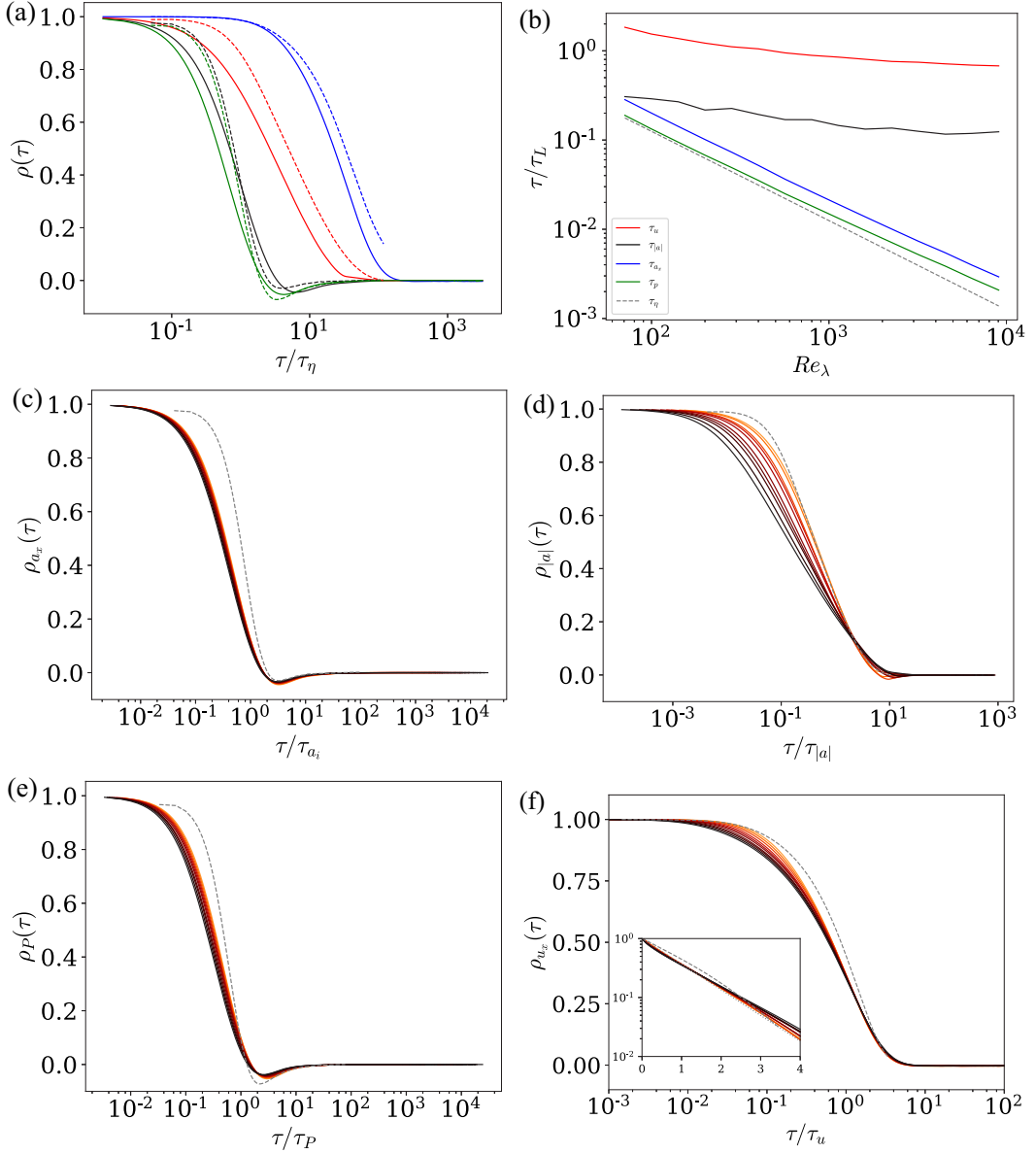
FIG. 10. (a) Evolution of the autocorrelation of a_i (black), $(a^2)^{1/2}$ (red), u_i (blue), and $P = a_i u_i$ (green) from the stochastic model for $Re_\lambda = 400$ and comparison with the DNS data from Ref. [61] in dashed lines. (b) Evolution of the integral timescale of a_i (black), $(a^2)^{1/2}$ (red), u_i (blue) and $P = a_i u_i$ (green) normalized by τ_L with the Reynolds number. (c, d, e, f) Evolution of the autocorrelation of a_i, $(a^2)^{1/2}$, $P = a_i u_i$ and u_i, respectively, for $Re_\lambda = 400$, 567, 800, 1130, 1600, 2263, 3200, 4526, 6400, and 9051 from orange to black and comparison with the DNS data from Ref. [61] in dashed lines. In these plots the time lag is normalized by the corresponding integral timescale. For panel (f), inset: logarithmic scaling of the y axis and comparison with $\exp(-\tau/\tau_u)$ in dotted line.

The shape of the velocity correlation from the model is overall close to the DNS. At small τ, it presents some dependence on the Reynolds number, while at large time shift (i.e., τ of the order of τ_L) the correlation decreases exponentially, as it can be seen in the inset of Fig. 10(f), in agreement
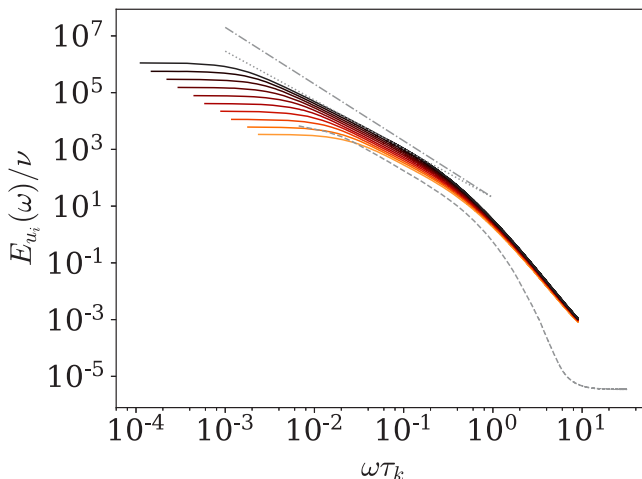
FIG. 11. Velocity spectra from the stochastic model for $Re_\lambda = 400$ to $Re_\lambda = 9000$ from orange to black and comparison with the DNS data from Ref. [61] at $Re_\lambda = 400$ (gray dashed line), with the Hinze spectra ω^{-2} (gray dot-dashed line), and with the power law with anomalous exponent $\omega^{-2+9/64}$ (gray dotted lines).

with DNS and experiments. The exponential relaxation results from the terms $P + K/\tau_\varepsilon = dK/dt + K/\tau_\varepsilon$ appearing in the drift part of the stochastic model (53). It is interesting to remark that the presence of this term in the model is a direct consequence of the exponential dependence of the conditional acceleration variance on the kinetic energy (22). This term leads to the Reynolds number dependence on the velocity correlation observed at small τ, which is connected to the logarithmic decorrelation of the acceleration norm, to vanish at large τ at which it relaxes exponentially. This suggests therefore anomalous scaling at intermediate time lag.

We show in Fig. 11 the velocity spectrum for Re_λ between 400 and 9000, which we compare with the DNS of Ref. [61] for $Re_\lambda = 400$. We see a good agreement between the DNS and the stochastic model. For higher Reynolds numbers, we clearly see that a power-law behavior develops at intermediate scales. We see that the slope of the power law deviates from the Hinze spectra [87] predicted by dimensional arguments similar to those presented by Kolmogorov, with spectra less stiff than ω^{-2}. This shows that the proposed stochastic model leads to an anomalous scaling that reflects the persistent influence of the Reynolds number in the inertial-scales. We further notice that the slope that develops at intermediate scales are close to $-2 + 0.14$, where 0.14 is the exponent of the asymptotic power law of the acceleration variance with the Reynolds number determined in Eq. (21) (see also Fig. 9). We see here a confirmation of the relation between the acceleration scaling and the anomalous scaling of the velocity spectra proposed by Ref. [26].

We present in Fig. 12 the PDFs of the velocity and of the acceleration for $Re_\lambda = 400 \sim 9000$, as well as the comparison with the DNS of Ref. [61]. First, we find that the velocity distribution is very close to a Gaussian distribution for all Reynolds numbers, while the acceleration presents a much more stretched distribution. For $Re_\lambda = 400$ the acceleration PDF is in very good agreement with the DNS, and, the model predicts an increase of the stretching of the tails with increasing the Reynolds number. We also show in this figure the PDF of the velocity increments for different time shifts $\delta_\tau u_i = u_i(t + \tau) - u_i(t)$ at $Re_\lambda = 400$. We observe that the distribution gradually returns to a Gaussian distribution as the time shift increases, and that at each time shift the agreement with the DNS of Ref. [61] is very good. This is confirmed by the presentation of the flatness of the velocity increments for $Re_\lambda = 400 \sim 9000$, which reflects the strongly non-Gaussian behavior on small scales which decreases to 3 for the larger scales. Here also we notice a good agreement with the DNS of Ref. [61] for $Re_\lambda = 400$. We also show in the inset, a quasilinear increase of the flatness of the acceleration with the Reynolds number.
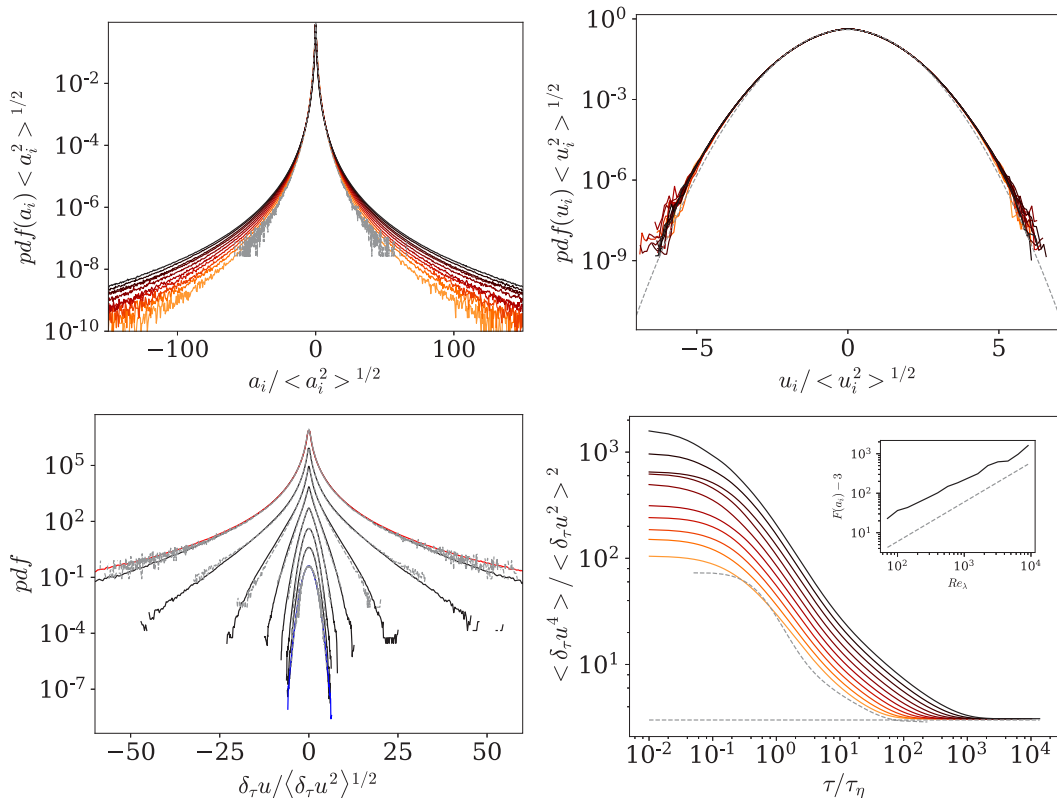
FIG. 12. PDF of a_i (top left) and comparison with the DNS data from Ref. [61], and PDF of u_i (top right) and comparison with the normal distribution, for $Re_\lambda = 400$ to 9000 from orange to black. (Bottom left) PDF of the velocity increments for various times shift: $\tau/\tau_\eta = 610, 200, 70, 22, 7.3, 2.4, 0.8,$ and 0.25 each time lag is shifted upward by one decade for $Re_\lambda = 400$ comparison with the PDF of the acceleration from the model (red) and from the DNS of Ref. [61] (gray) and the PDF velocity (blue). (Bottom right) Evolution of the Flatness of the velocity increments versus the time shift for $Re_\lambda = 70$ to 9000 from orange to black and evolution of the flatness of the acceleration with the Reynolds number and comparison with the linear law in the inset.

Finally, in Fig. 13 we show the second and third moments of the power $P = a_i u_i$. It is observed that the increases of both moments with the Reynolds number are in close agreement with the power law supported by the DNS results of Ref. [28], $\langle P^2 \rangle / \langle \varepsilon \rangle^2 \sim Re_\lambda^{4/3}$ and $-\langle P^3 \rangle / \langle \varepsilon \rangle^3 \sim Re_\lambda^2$. Clearly, the third-order moment is negative, meaning that the time irreversibility of the dynamics of a fluid particle in a turbulent flow is correctly reproduced by the proposed stochastic model. The skewness of the power, $S = \langle P^3 \rangle / \langle P^2 \rangle^{3/2}$, seems to converge to -0.5 as the Reynolds number increases, as reported in Ref. [28].

IV. DISCUSSION AND FINAL REMARKS

In this paper, we have analyzed the behavior of the acceleration statistics conditioned on both local dissipation rate and local kinetic energy, which to our knowledge have not been considered before. We have reported that the doubly conditional variance is proportional to the acceleration variance conditional on the dissipation rate solely, with the proportionality factor depending exponentially on the kinetic energy: $\langle a^2 | \varepsilon, K \rangle = A \exp(\alpha K / \langle K \rangle) \langle a^2 | \varepsilon \rangle$. For large enough Reynolds
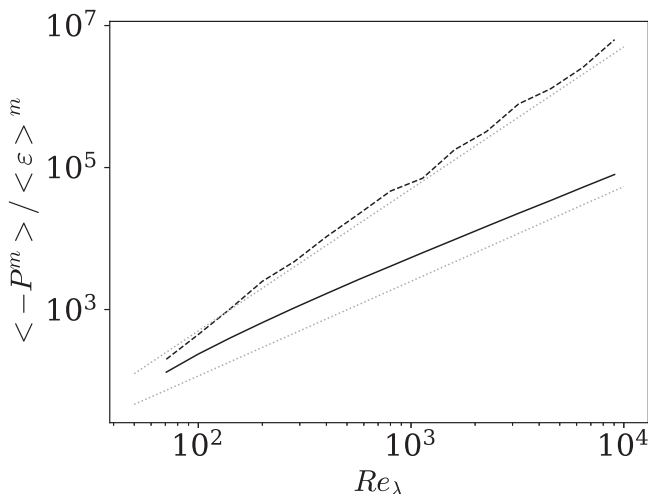
FIG. 13. Evolution of $\langle P^2 \rangle / \langle \varepsilon \rangle^2$ (continuous black line) and $-\langle P^3 \rangle / \langle \varepsilon \rangle^3$ (dashed black line) with the Reynolds number, and comparison with the power laws $\mathrm{Re}_\lambda^{4/3}$ and Re_λ^2.

number we show that $A = (1 - 2\alpha/3)^{3/2}$ and we proposed that the α coefficient is independent of the Reynolds number and its value $\alpha = 1/3$ was obtained from the DNS.

This expression shows a direct effect of the kinetic energy, a large-scale quantity, on the Lagrangian acceleration. Furthermore since the argument of the exponential depends on $K/\langle K \rangle$, not on a local Reynolds number, it suggests a kinematic effect for the acceleration which may be due to the nonlocality of the pressure. More specifically, these effects can be due to the interaction of vorticity and strain [29]. In case of persistent large-scale strain, intense vorticity tube would be generated and align with the principal direction of the strain [88]. It was shown that such vortical structure can produce significant acceleration in the direction of the vorticity [52,89]. Anyway, although the proper physical mechanism leading to the exponential dependence of the acceleration on the kinetic energy deserve further studies it is an additional effect to the influence of the large scales on the acceleration through the intermittency of the dissipation rate. To study this later effect, we subsequently have proposed to account for the Reynolds number dependence of the acceleration variance conditional on the dissipation rate within the intermediate asymptotic framework [65] leading to: $\langle a^2 | \varepsilon \rangle = a_\eta^2 B(\varepsilon / \langle \varepsilon \rangle)^{3/2+\beta}$ for $\varepsilon \gg \langle \varepsilon \rangle$ with B and β depending logarithmically on the Reynolds number as the signature of the intermittency and the persistence of viscous effects. Further, we advance an expression for the conditional acceleration variance valid for the whole range of fluctuations of ε by accounting for the dominant effect of the large-scale structures in low dissipative regions [see Eq. (16)]. From this finding we determine the evolution of the unconditional acceleration variance with the Reynolds number [Eq. (20)] and show that it is in good agreement with DNS, which gives another empirical validation of the incomplete similarities assumption used to obtain these results.

Eventually, for large Reynolds numbers, we propose to express the doubly conditional variance as $\langle a^2 | \varepsilon, K \rangle = Ca_\eta^2 \exp(\alpha K / \langle K \rangle + \gamma \ln \varepsilon \langle \varepsilon \rangle)$, $\gamma = 3/2 + \beta$, which can be viewed as the results of a multiplicative process for the acceleration. Such process can be interpreted as a momentum fluctuation cascade that includes kinematic effects by eddies all along the turbulence spectrum.

Based on these results we propose a 3D stochastic model for the dynamics of a fluid particle that reproduce the essential features of the Lagrangian dynamics observed from DNS and experiments. To obtain such model, (i) we have assumed, inline with the Kolmogorov universality hypothesis, that the dynamics can be described as a set of stochastic differential equation $da_i = M_i dt + D_{ij} dW_j$; $du_i = a_i dt$, with M_i and D_{ij} depending on the velocity and acceleration along with Reynolds number

dependent parameters. (ii) We used the doubly conditional acceleration variance obtained in this paper, to model the instantaneous relation of the dynamics between acceleration (or force), kinetic energy, and energy dissipation. This amounts to consider that the remaining degree of freedom can be discarded in procedure similar to an adiabatic elimination [90] as discussed by Ref. [70]. (iii) We introduce a nondiagonal diffusion tensor along with a maximum winding hypothesis to ensure its physical realizability. (iv) We consider that the dissipation rate along the trajectory is given by the non-Markovian log-normal process proposed recently by Ref. [81], giving logarithmic correlation consistently with the turbulent cascade picture. The model is closed by using the relation $dK/dt = P = a_i u_i$. For the model, it implies dependence of K on ε through the dependence of a^2 on ε. This can be interpreted as feedback of the small scales on the large scales. Additionally, the influence of the large scales on the small scales is accounted for in the model through the intermittent cascade model for the dissipation rate. With these four hypotheses, we obtain the model given by Eqs. (31), (32), (54), and (55), which reads

$$da_i = \left[\frac{\alpha}{2\langle K \rangle} \left(a_i \left(c_u P + \frac{K}{\tau_\varepsilon} \right) - (c_u - 1)a^2 u_i \right) - a_i \left(\ln \left(\frac{a^2}{a_\eta^2} \right) + \hat{\Gamma}_* \right) \frac{1}{2\tau_\varepsilon} - \frac{\sigma_*^2}{\tau_c} \frac{a_T^2}{a^2} a_i \right] dt$$
$$+ \sqrt{\frac{\sigma_*^2}{\tau_c}} \left[\sqrt{a_T^2} \delta_{ij} + \sqrt{a_N^2} \epsilon_{ijk} b_k \right] dW_j. \tag{56}$$

We show that the proposed model predicts Lagrangian dynamics presenting non-Gausssianity, long-range correlations, anomalous scaling, and time irreversibility. Moreover, statistics obtained from the stochastic model are in good agreement with the DNS.

In Eq. (56) the term proportional to α, which follows directly from the exponential dependence of the conditional acceleration on the kinetic energy, involves the coupling between velocity and acceleration and leads to the exponential relaxation of the velocity correlation for large time lag along with one-time Gaussian distribution for the velocity. Introducing a rotational part in the diffusion tensor naturally leads to decomposition of the acceleration vector into its tangential part and its normal components. Since the normal part is associated with the curvature of the trajectory, the rotational part of the diffusion leads to the emergence of a timescale separation between the correlation of the norm and the components of the acceleration. The term associated with the non-Markovianity of the dissipation along with the rotational part produce irreversible dynamics, as seen by the skewness of the exchanged power and ensures a scale separation between velocity and acceleration. These three points can be easily checked, by taking $\alpha = 0$ or $c_R = 0$ in Eq. (41) or by using for Π the Markovian log-normal dissipation model proposed by Ref. [40] rather than the non-Markovian one of Ref. [81].

It is worth noting that from the conditional acceleration statistics obtained from DNS of the Navier-Stokes equation, it is possible to establish, in a fairly natural way, that is to say without using any other hypothesis than the cascade picture, a link between the refined Kolmogorov assumption and the dynamics of fluid particles. It would be interesting to analyze further the stochastic equation to demonstrate the irreversibility of the dynamics, the emergence of anomalous scaling or to study the geometry of the particle trajectory e.g. its curvature and torsion, as well as to further test the conditional statistics between the acceleration and the velocity. Also interesting could be the improvement of the modeling of the high frequency part of the spectrum. Indeed, the dissipative part of the spectrum is not well reproduced by the model of Ref. [81] which intends to model the dissipation rate in the inertial range.

To simplify the construction of the model, we have not taken into account the nonlocal effects of the largest structures of the flow, arguing that their effect vanish as the Reynolds number increases [term with a_0^2 in Eq. (16)]. Based on the relation (16) it is possible to account for the large scale in the stochastic modeling. However, since this term is dependent on the Reynolds number, it is likely that it also depends on the flow configuration and boundary conditions. The proposed stochastic model could be further generalized to address shear flows [52] and improve Reynolds-averaged simulations

[91,92]. This model could be used among other things to improve the calculation of the dynamics of a dispersed phase with the large eddy simulation (LES) approach [54,57,93]. Finally, let us mention that an interesting extension could be the coupling of the proposed model with stochastic model for the evolution of the velocity gradients as proposed in Refs. [77,78,94,95].

APPENDIX A: ESTIMATION OF c_ε

To evaluate the c_ε factor appearing in Eq. (1), we use the following relation between the conditional averages[3]:

$$\langle a^2|\varepsilon\rangle = \int dK \langle a^2|\varepsilon, K\rangle P(K|\varepsilon). \tag{A1}$$

Substituting relation (1) in Eq. (A1), we find, assuming that c_ε is independent of K,

$$\langle a^2|\varepsilon\rangle/a_\eta^2 = c_\varepsilon \int dK \exp(\alpha K/\langle K\rangle)P(K|\varepsilon). \tag{A2}$$

If the kinetic energy is statistically independent of the dissipation rate [i.e., $P(K|\varepsilon) = P(K)$] the integral in the previous relation takes a constant value and c_ε is proportional to $\langle a^2|\varepsilon\rangle$. However, such an assumption is only approximate at moderate Reynolds numbers as shown from our DNS. Indeed, it is seen in Fig. 14 that the average of K conditioned on ε has a weak logarithmic dependence on ε. Note that the average dissipation rate conditional on the kinetic energy can be found in Ref. [96]. We also present in Fig. 14 the probability density of the kinetic energy conditioned on the dissipation rate. In this figure, the PDF is normalized by its mean value $\langle K|\varepsilon\rangle$. It is notable that for large values of the dissipation rate, the conditional PDF takes a self-similar form:

$$P(K/\langle K|\varepsilon\rangle|\varepsilon) = P_G(K/\langle K|\varepsilon\rangle). \tag{A3}$$

Thus, by combining the previous relations, one can write

$$\langle a^2|\varepsilon\rangle/a_\eta^2 = c_\varepsilon \int dK^* \exp(\alpha^* K^*)P_G(K^*), \tag{A4}$$

where we have introduced $K^* = K/\langle K|\varepsilon\rangle$ and $\alpha^*(\varepsilon) = \alpha \langle K|\varepsilon\rangle/\langle K\rangle$. In addition, we see in Fig. 14 that the self-similar form of the distribution of K^* knowing ε is well approximated by the following distribution obtained from the Maxwell distribution (i.e., assuming that the three components of the velocity are Gaussian and independent):

$$P_G(x) = \frac{3}{\sqrt{\pi}}\sqrt{\frac{3}{2}x} \exp\left(-\frac{3}{2}x\right). \tag{A5}$$

---

[3]This relation is simply obtained from the relation between the joint PDF and the conditional PDF: $P(a^2, \varepsilon, K) = P(a^2|\varepsilon, K)P(\varepsilon, K) = P(a^2|\varepsilon, K)P(K|\varepsilon)P(\varepsilon)$ and the relation between the joint probability density of a^2, ε, K and a^2, ε: $P(a^2, \varepsilon) = \int dKP(a^2, \varepsilon, K)$.
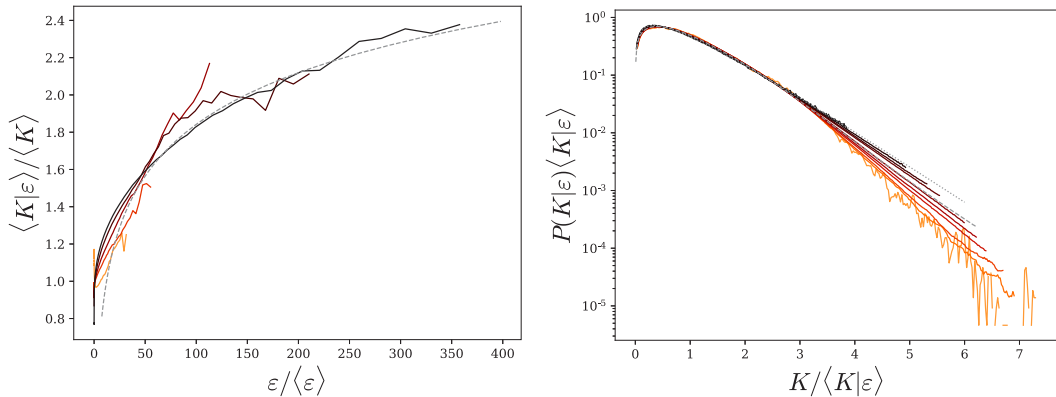
FIG. 14. (Left) Average of the kinetic energy conditioned on the local dissipation rate from our DNS for $Re_\lambda = 50, 90, 150, 230$, and 380 in continuous lines from orange to black, respectively, and comparison with the relation $\langle K|\varepsilon\rangle/\langle K\rangle = 0.4\ln(\varepsilon/\langle\varepsilon\rangle)$. (Right) Probability density function of the kinetic energy conditioned on the dissipation rate, normalized by its average $\langle K|\varepsilon\rangle$, from our DNS at $Re_\lambda = 380$ for $\varepsilon/\langle\varepsilon\rangle = 0.01, 0.05, 0.1, 0.3, 0.5, 1, 3, 5, 10, 50 \pm 30\%$ from orange to black. Comparison with the marginal PDF of the kinetic energy in dashed line and with the PDF (A5) in dotted line.

Note that the average of this distribution is indeed unity: $\int x P_G(x)dx = 1$. With this expression for P_G the integral of Eq. (A4) can be computed as

$$A_\varepsilon^{-1} = \int dK^* \exp(\alpha^* K^*)P_G(K^*) = \left(1 - \frac{2}{3}\alpha^*\right)^{-3/2}. \tag{A6}$$

Thus, according to Eq. (A2), we have for c_ε

$$c_\varepsilon = A_\varepsilon \langle a^2|\varepsilon\rangle/a_\eta^2. \tag{A7}$$

The dependence of A_ε with ε explains the deviation of the power-law behavior between $\langle a^2|\varepsilon, K\rangle$ and $\langle a^2|\varepsilon\rangle$ observed in Fig. 2(b) for $\varepsilon \gg \langle\varepsilon\rangle$.

It is notable that the integral A_ε converges only if $\alpha^* < 3/2$. This observation suggests that the dependence of $\langle K|\varepsilon\rangle/\langle K\rangle$ on ε should decrease as the Reynolds number increases to allow α^* to remains lower than $3/2$ even for the most intense fluctuations of $\varepsilon/\langle\varepsilon\rangle$, and thus ensuring the convergence of the integral. Therefore, the larger the Reynolds number, the weaker the dependence of $\langle K|\varepsilon\rangle/\langle K\rangle$ on ε. This is consistent, with the statistical independence between the local values of the kinetic energy and of the dissipation at large Reynolds numbers, in line with scale separation of the turbulent cascade. Accordingly, we simply propose to write

$$c_\varepsilon \approx A \langle a^2|\varepsilon\rangle/a_\eta^2, \tag{A8}$$

where $A = (1 - \frac{2}{3}\alpha)^{3/2}$, which is equal to $A = 7\sqrt{7}/27 \approx 0.686$, for $\alpha = 1/3$, neglecting the small logarithmic dependence in $\varepsilon/\langle\varepsilon\rangle$.

APPENDIX B: ANALYTICAL ESTIMATION OF THE ACCELERATION VARIANCE

Using expression (16) for the conditional acceleration variance, we write the acceleration variance as

$$\frac{\langle a^2\rangle}{a_\eta^2} = B \int_0^\infty (Z + \varepsilon_*)^\gamma P(\varepsilon_*)d\varepsilon_*, \tag{B1}$$

where we introduced $\gamma = 3/2 + \beta$, $Z = (\frac{1}{B}\frac{a_0^2}{a_\eta^2})^{1/\gamma}$ and $\varepsilon_* = \varepsilon/\langle\varepsilon\rangle$ for simplicity. We can expand the term within the integral using the generalized binomial series:

$$(Z + \varepsilon_*)^\gamma = \begin{cases} \sum_{k=0}^{\infty} C_{\gamma,k} Z^{\gamma-k}\varepsilon_*^k & \text{for} \quad \varepsilon_* < Z, \\ \sum_{k=0}^{\infty} C_{\gamma,k} Z^k \varepsilon_*^{\gamma-k} & \text{for} \quad \varepsilon_* > Z, \end{cases} \tag{B2}$$

with $C_{\gamma,k} = \binom{\gamma}{k} = \frac{1}{k!}\prod_{i=0}^{k-1}(\gamma - i)$ the generalized binomial coefficient. In particular, we have $C_{\gamma,0} = 1$ and $C_{\gamma,1} = \gamma$. Splitting the integral in Eq. (B1) enables us to write

$$\frac{\langle a^2 \rangle}{a_\eta^2} = B\sum_{k=0}^{\infty} C_{\gamma,k}\left[Z^{\gamma-k}\int_0^Z \varepsilon_*^k P(\varepsilon_*)d\varepsilon_* + Z^k \int_Z^\infty \varepsilon_*^{\gamma-k}P(\varepsilon_*)d\varepsilon_*\right]. \tag{B3}$$

The two integrals are partial moments of the normalized dissipation rate. Considering that ε_* follows the log-normal distribution with parameters μ and σ^2, with the change of variable $x = (\ln\varepsilon_* - \mu)/\sqrt{\sigma^2}$, we can express the partial moments of order n as

$$\int_Z^\infty \varepsilon_*^n P(\varepsilon_*)d\varepsilon_* = \exp(n\mu + n^2\sigma^2/2)\int_{(\ln Z - \mu)/\sqrt{\sigma^2}}^\infty \exp(-(x - n\sqrt{\sigma^2})^2/2)dx = \langle\varepsilon_*^n\rangle\Phi(Z, n), \tag{B4}$$

with $\Phi(Z, n) = \frac{1}{2} - \frac{1}{2}erf(\frac{\ln Z - \mu}{\sqrt{2\sigma^2}} - \frac{n\sqrt{\sigma^2}}{\sqrt{2}})$. Note that since $\langle\varepsilon_*\rangle = 1$, we have $\mu = -\sigma^2/2$ which gives for the regular moments $\langle\varepsilon_*^n\rangle = \exp(\sigma^2 n(n-1)/2)$ and $\Phi(Z, n) = \frac{1}{2} - \frac{1}{2}erf[\frac{\ln Z + \sigma^2(n-1/2)}{\sqrt{2\sigma^2}}]$. As well, we have for the other partial moments

$$\int_0^Z \varepsilon_*^n P(\varepsilon_*)d\varepsilon_* = \langle\varepsilon_*^n\rangle[1 - \Phi(Z, n)]. \tag{B5}$$

For the acceleration variance, we obtain eventually the following analytical series expansion

$$\frac{\langle a^2 \rangle}{a_\eta^2} = B\sum_{k=0}^{\infty} C_{\gamma,k}\{Z^{\gamma-k}\langle\varepsilon_*^k\rangle[1 - \Phi(Z, k)] + Z^k\langle\varepsilon_*^{\gamma-k}\rangle\Phi(Z, \gamma - k)\}. \tag{B6}$$

This expression is observed to converge very rapidly to the numerical evaluation of the integral (B1), as there is just minute differences when considering only the first three elements of the sum.

For Z and k small, we have $\Phi(Z, k) = O(1)$, which allow us to simplify the relation for the acceleration variance:

$$\frac{\langle a^2 \rangle}{a_\eta^2} = B\sum_{k=0}^{\infty} C_{\gamma,k}Z^k\langle\varepsilon_*^{\gamma-k}\rangle. \tag{B7}$$

The successive terms of the series correspond to corrections of low-Reynolds number effects of increasingly high order, since $Z \sim \text{Re}_\lambda^{-1/\gamma}$. At leading order we have

$$\frac{\langle a^2 \rangle}{a_\eta^2} = B\langle\varepsilon_*^\gamma\rangle, \tag{B8}$$

while the first-order correction gives

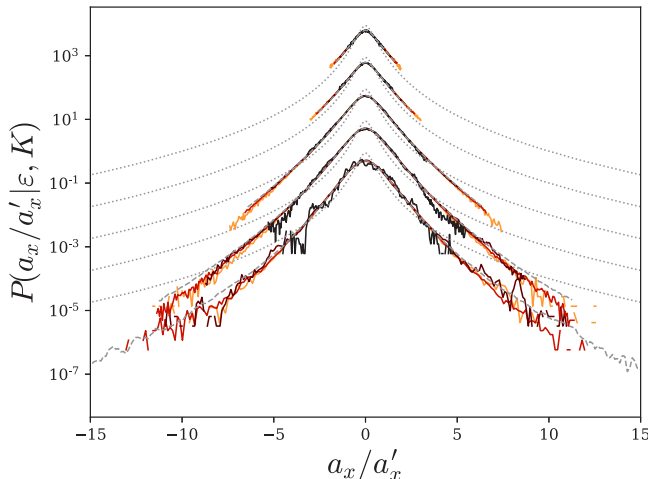$$\frac{\langle a^2 \rangle}{a_\eta^2} = B(\langle\varepsilon_*^\gamma\rangle + \gamma Z\langle\varepsilon_*^{\gamma-1}\rangle). \tag{B9}$$

FIG. 15. PDF of the acceleration conditional on the dissipation and the kinetic energy $P(a_i|\varepsilon, K)$ for various values of ε and K: $K/\langle K \rangle = 0.1$, 1, 2.5, and $5 \pm 30\%$ from orange to black, respectively, and $\varepsilon/\langle \varepsilon \rangle = 0.05$, 0.3, 1, 5, and $10 \pm 30\%$ shifted, respectively, by one decade upward. Comparison with the acceleration PDF conditioned only by the dissipation in gray dashed line, and with the unconditional PDF in dotted gray line. Each PDF is normalized by its standard deviation. Data from our DNS at $\mathrm{Re}_\lambda = 380$.

With $\sigma^2 = 3/8 \ln \mathrm{Re}_\lambda/R_c$ as proposed by Ref. [12], the leading order expression (B8) gives Eq. (19), and the first-order expression reads

$$\frac{\langle a^2 \rangle}{a_\eta^2} = B\left(\frac{\mathrm{Re}_\lambda}{R_c}\right)^{3/16\gamma(\gamma-1)}\left[1 + \gamma\left(\frac{1}{B}\frac{a_0^2}{a_\eta^2}\right)^{1/\gamma}\left(\frac{\mathrm{Re}_\lambda}{R_c}\right)^{-3/8(\gamma-1)}\right]. \tag{B10}$$

This later expression is seen in Fig. 9 to give a very good approximation of Eq. (16).

APPENDIX C: CONDITIONAL PDF OF THE ACCELERATION

We complete the statistical description of the conditional acceleration by showing, in Fig. 15, its probability density function (PDF). In this figure, we compare the PDF of the acceleration conditional on the dissipation and the kinetic energy, with the PDF conditioned only by the dissipation and with the unconditional PDF obtained from our DNS at $\mathrm{Re}_\lambda = 380$. All the PDFs are normalized by their respective standard deviation. It is observed that the conditional PDFs present much less developed tails than the unconditional PDF. Moreover, the doubly conditional PDFs overlap with the simply conditional PDF, showing that conditioning by the velocity does not alter the shape of the PDF. As well the shape is observed to be invariant for all values of ε, supporting the idea of a canonical distribution presented in Ref. [97].

APPENDIX D: MODELING OF THE DISSIPATION RATE

1. Dissipation as multiplicative cascade process

The image of the energy cascade is naturally associated with multiplicative processes [49,71–75]. Such model proposes to express the locally space-averaged dissipation over a volume of size $\ell = L\lambda^n$, with L the large scale of the flow and $\lambda < 1$, as

$$\varepsilon_n = \varepsilon_0 \frac{\varepsilon_1}{\varepsilon_0} \cdots \frac{\varepsilon_n}{\varepsilon_{n-1}} = \varepsilon_0 \prod_{i=1}^{n} \xi_i. \tag{D1}$$

Assuming that $\xi_i = \varepsilon_i/\varepsilon_{i-1}$ are independent positive random numbers with identical distribution across scales we write

$$\ln \frac{\varepsilon_n}{\varepsilon_0} = \sum_{i=1}^{n} \ln \xi_i. \tag{D2}$$

Therefore, according to the central limit theorem the term on the right must present a normal distribution with parameters $\mu = n\mu_\xi$ and $\sigma^2 = n\sigma_\xi^2$. The parameters μ_ξ and σ_ξ^2 appear as fundamental unknowns, but can nevertheless be related with the relation $\mu_\xi = -\sigma_\xi^2/2$ obtained from the moments of a log-normal variable to guarantee that the average energy flux is conserved throughout the cascade. Setting $\ell = \eta$ (i.e. $n = \ln(\eta/L)/\ln \lambda \sim \ln \mathrm{Re}_\lambda$) we obtain a model for the local dissipation rate. The log-normal distribution for ε has been confirmed, for example, by DNS of Ref. [12]. Moreover, for the variance of the logarithm of the local dissipation rate is then $\sigma^2 = \frac{\sigma_\xi}{\ln \lambda} \ln \eta/L = A + B \ln \mathrm{Re}_\lambda$ as predicted by Kolmogorov and Oboukhov [35,69]. Such evolution for σ^2 has been also confirmed by the DNS of Ref. [12] showing that $\sigma^2 \approx 3/8 \ln \mathrm{Re}_\lambda/10$.

Such multiplicative process also implies a logarithmic evolution of the spatial correlation of the dissipation rate as explained by Mandelbrot [98]. We consider the dissipation rate at two points A and B, ε_n^A and ε_n^B, both defined on the same scale n. The points A and B are separated by a distance $L > r > \eta$ from each other and we note $k = \ln(r/L)/\ln \lambda$, then $0 < k < n$. Clearly, the greater the distance between the two points, the larger the scale of their common root in the cascade:

$$\varepsilon_n^A = \varepsilon_0^{AB} \frac{\varepsilon_1^{AB}}{\varepsilon_0^{AB}} \cdots \frac{\varepsilon_k^{AB}}{\varepsilon_{k-1}^{AB}} \frac{\varepsilon_{k+1}^A}{\varepsilon_k^A} \cdots \frac{\varepsilon_n^A}{\varepsilon_{n-1}^A}, \tag{D3}$$

$$\varepsilon_n^B = \varepsilon_0^{AB} \frac{\varepsilon_1^{AB}}{\varepsilon_0^{AB}} \cdots \frac{\varepsilon_k^{AB}}{\varepsilon_{k-1}^{AB}} \frac{\varepsilon_{k+1}^B}{\varepsilon_k^B} \cdots \frac{\varepsilon_n^B}{\varepsilon_{n-1}^B}. \tag{D4}$$

In the two previous equations, we have distinguished by the exponents A and B the variables which are specific to points A and B and by AB those which are common. This can be expressed as

$$\ln \frac{\varepsilon_n^A}{\varepsilon_0} = \sum_{i=1}^{k} \ln \xi_i^{AB} + \sum_{i=k+1}^{n} \ln \xi_i^A, \tag{D5}$$

$$\ln \frac{\varepsilon_n^B}{\varepsilon_0} = \sum_{i=1}^{k} \ln \xi_i^{AB} + \sum_{i=k+1}^{n} \ln \xi_i^B. \tag{D6}$$

The correlation between $\ln \varepsilon_n^A$ and $\ln \varepsilon_n^B$ is defined as

$$R_{\ln \varepsilon}(r) = \left\langle \left(\ln \frac{\varepsilon_n^A}{\varepsilon_0} - \mu \right) \left(\ln \frac{\varepsilon_n^B}{\varepsilon_0} - \mu \right) \right\rangle = \left\langle \ln \frac{\varepsilon_n^A}{\varepsilon_*} \ln \frac{\varepsilon_n^B}{\varepsilon_*} \right\rangle, \tag{D7}$$

where we noted $\varepsilon_* = \varepsilon_0 e^\mu$. Introducing similarly $\xi_* = e^{\mu_\chi}$ and $\xi' = \xi/\xi_*$ we express the correlation as

$$
\begin{aligned}
R_{\ln \varepsilon} &= \left\langle \sum_{i=1}^{n} \left(\ln \xi_i^A - \mu_\xi \right) \sum_{j=1}^{n} \left(\ln \xi_i^B - \mu_\xi \right) \right\rangle = \left\langle \sum_{i=1}^{n} \ln \xi_i'^A \sum_{j=1}^{n} \ln \xi_j'^B \right\rangle \\
&= \left\langle \left(\sum_{i=1}^{k} \ln \xi_i'^{AB} + \sum_{i=k+1}^{n} \ln \xi_i'^A \right) \left(\sum_{j=1}^{k} \ln \xi_j'^{AB} + \sum_{j=k+1}^{n} \ln \xi_j'^B \right) \right\rangle \\
&= \sum_{i=1}^{k} \sum_{j=1}^{k} \left\langle \ln \xi_i'^{AB} \ln \xi_j'^{AB} \right\rangle + \sum_{i=1}^{k} \sum_{j=k+1}^{n} \left\langle \ln \xi_i'^{AB} \ln \xi_j'^{AB} \right\rangle
\end{aligned}
$$

$$+ \sum_{i=k+1}^{n} \sum_{j=1}^{k} \left\langle \ln \xi_i'^A \ln \xi_j'^{AB} \right\rangle + \sum_{i=k+1}^{n} \sum_{j=k+1}^{n} \left\langle \ln \xi_i'^{AB} \ln \xi_j'^B \right\rangle$$

$$= \sum_{i=1}^{k} \sum_{j=1}^{k} \delta_{ij} \sigma_\xi^2 = k \sigma_\xi^2. \tag{D8}$$

To obtain this result we used the hypothesis that within the same branch the events at a given scale are independent of those at another scale, $\langle \ln \xi_i'^{AB} \ln \xi_j'^{AB} \rangle = \delta_{ij} \sigma_\xi^2$, as well as vanishing correlation between branches A and B: $\langle \ln \xi_i'^A \ln \xi_j'^B \rangle = 0$. This gives a logarithmic evolution of the correlation coefficient $\rho_{\ln \varepsilon} = R_{\ln \varepsilon} / \sigma^2$, in the range $\eta < r < L$:

$$\rho_{\ln \varepsilon} = \frac{\left\langle \ln \frac{\varepsilon_n^A}{\varepsilon_*} \ln \frac{\varepsilon_n^B}{\varepsilon_*} \right\rangle}{\left\langle \ln^2 \frac{\varepsilon_n}{\varepsilon_*} \right\rangle} = \frac{k}{n} = \frac{\ln L/r}{\ln L/\eta} = 1 - \frac{\ln r/\eta}{\ln L/\eta}. \tag{D9}$$

Although not trivial, this result can be transposed for the temporal correlation along particle path [99–102]. The logarithmic behavior of the correlation is confirmed by DNS, as it can be seen in Ref. [82] where the evolution of the Lagrangian correlation of the logarithm of the dissipation is presented.

2. Stochastic modeling of the dissipation

It has been proposed to model the dissipation rate as stochastic multiplicative process. Such process can be generically expressed as

$$d\varepsilon = \varepsilon \Pi dt + \varepsilon \Sigma dW, \tag{D10}$$

with dW the increment of the Wiener process ($\langle dW = 0$ and $\langle dW^2 \rangle = dt$) and where Π and Σ are to be determined.

Considering that ε follows a log-normal distribution with parameter σ^2 and $\mu = -\sigma^2/2$, we define the standard normal variable χ (Gaussian random variable with zero mean and unit variance) as

$$\frac{\varepsilon}{\langle \varepsilon \rangle} = \exp(\sigma \chi - \sigma^2/2). \tag{D11}$$

A stochastic process for χ has to be given to obtain the stochastic process for ε, via the Ito transformation.

Pope and Chen [40] proposed to obtain χ from an Orstein-Uhnlebbeck process with a characteristic time τ_ε:

$$d\chi = -\frac{\chi}{\tau_\varepsilon} dt + \sqrt{\frac{2}{\tau_\varepsilon}} dW. \tag{D12}$$

According to the Ito formula, this gives for Π and Σ

$$\Pi = -(\ln \varepsilon/\langle \varepsilon \rangle - \sigma^2/2)/\tau_\varepsilon, \tag{D13}$$

$$\Sigma = \sqrt{2\sigma^2/\tau_\varepsilon}. \tag{D14}$$

This process gives as expected log-normal distribution for ε (normal distribution for χ) as well as an exponential decrease of the correlation of $\ln \varepsilon$ with a characteristic time τ_ε. This exponential behavior is not consistent with the multiplicative cascade model as discuss above. It rather corresponds to a direct energy transfer from large to small scales.
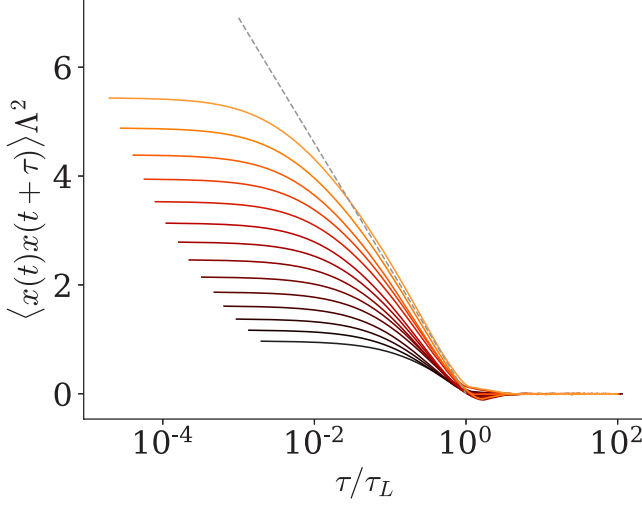
FIG. 16. Correlation of χ for various values of $\tau_\varepsilon / \tau_c$.

To ensure a logarithmic decorrelation of the dissipation, Chevillard [81] proposed to adapt the Gaussian multiplicative chaos introduced by Mandelbrot [98]. This leads to a multifractal model in which the increment of the Wiener process in Eq. (D12) is replaced by a fractional Gaussian noise:

$$d\chi = -\frac{\chi}{\tau_\varepsilon}dt + \frac{1}{\Lambda}dW_{\tau_c}^0, \tag{D15}$$

where $dW_{\tau_c}^0$ is formally a fractional Gaussian noise with a 0 Hurst exponent, regularized at a timescale τ_c, and Λ is a normalization factor ensuring unit variance for χ. The value of Λ is dependent on the specific regularization of $dW_{\tau_c}^0$. As explained in Ref. [81] this process can be reexpressed as

$$d\chi(t) = \left(-\frac{\chi}{\tau_\varepsilon} + \frac{\Gamma}{\Lambda}\right)dt + \frac{1}{\sqrt{\Lambda^2\tau_c}}dW, \tag{D16}$$

with dW the increments of a standard Wiener process and Γ corresponds to a convolution of the Wiener increments:

$$\Gamma = -\frac{1}{2}\int_{-\infty}^{t}(t - s + \tau_c)^{-3/2}dW(s), \tag{D17}$$

where $dW(s)$ is the increments of the same realization of the Wiener process as in Eq. (D16). In Eq. (D17), the regularization time τ_c prevent the divergence of the kernel when $s \rightarrow t$. The normalization factor Λ is estimated as $\Lambda = \langle X^2 \rangle$ where X obey the stochastic Eq. (D16) in which Λ has been set to 1.

The stochastic process (D16) gives a logarithmic correlation for χ: $\langle \chi(t)\chi(t - s) \rangle \sim \ln\frac{\tau_\varepsilon}{s}$ for $\tau_c \ll s \ll \tau_\varepsilon$, as illustrated in the Fig. 16.

With the Ito transformation, we obtain the process for ε from (D16). This gives for Π and Σ:

$$\Pi = \left(-\ln\frac{\varepsilon}{\langle\varepsilon\rangle} + \frac{\sigma^2}{2\Lambda^2}\left(\frac{\tau_\varepsilon}{\tau_c} - \Lambda^2\right) + \frac{\sigma}{\Lambda}\Gamma\tau_\varepsilon\right)\Big/\tau_\varepsilon, \tag{D18}$$

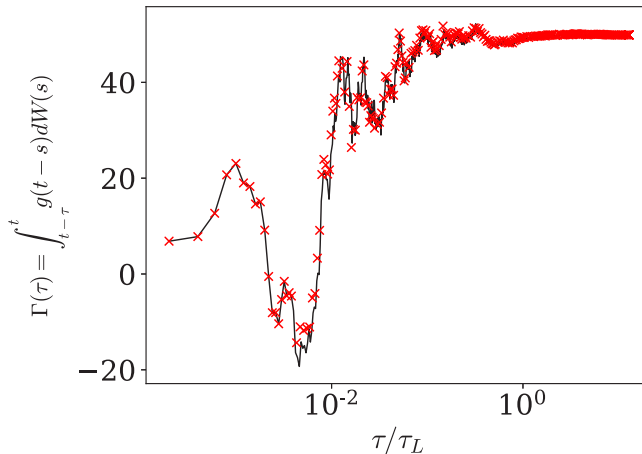$$\Sigma = \sqrt{\frac{\sigma^2}{\Lambda^2\tau_c}}. \tag{D19}$$

FIG. 17. One realization of the integral (D17) as a function of the lower bound of the integral for $dt = \tau_c/100$. Comparison between the direct calculation of the history integral (D17) (black line) and the optimized calculation with $N_s = 12$ (red crosses).

3. Efficient calculation of the stochastic convolution Γ

To obtain a stationary process the lower bound of the integration is set to $-\infty$. For the numerical computation of this integral, the lower limit has to be truncated. We present in Fig. 17 one realization of the evolution of the integral $\Gamma(t, \tau) = -\frac{1}{2} \int_{t-\tau}^{t} (t - s + \tau_c)^{-3/2} dW(s)$ when the lower bound varies. We see that for values larger than τ_ε the integral converges to a value (which remains random). In addition, the convergence threshold does not seem to depend on the time step used. So in practice Γ will be calculated with a lower-bound set to $t - 5\tau_\varepsilon$.

To obtain these calculations, the integral (D17) giving the value of Γ at time $t_n = n\,dt$ has been discretized as proposed by Ref. [81],

$$\Gamma_n = -\frac{1}{2} \sum_{m=0}^{N_{\text{hist}}} (s_m + \tau_c)^{-3/2} \, dW_{n-m}, \tag{D20}$$

with $s_m = t_n - t_{n-m} = m\,dt$, $N_{\text{hist}} = 5\tau_\varepsilon/dt$, and dW_{n-m} the increment of the Wiener process at time $(n-m)dt$.

This direct calculation requires a lot of memory to keep the last N_{hist} instants and requires a very large number of operations, of the order of $N_t \times N_{\text{hist}}$ where N_t is the number of time steps of the simulation. Thus, this direct method is difficult to use in practice when $\tau_\varepsilon/\tau_\eta \sim \text{Re}_\lambda$ becomes large.

For this reason, Ref. [81] proposed to speed up significantly the calculation using the fast Fourier transforms (FFT). The integral at time $n\,dt$ is then computed as $\Gamma_n = -1/2z_n$ where $z_n = FFT^{-1}(Z_k)$ is given by the inverse Fourier transform of Z_k. $Z_k = X_k Y_k$ is the convolution in spectral space between x_n and y_n [$X_k = FFT(x_n)$ and $Y_k = FFT(y_n)$], where x_n and y_n are the sequences dW_n and $(s_n + \tau_c)^{-3/2}$ padded with zeros such that they have $N > N_{\text{hist}} + N_t$ points. This algorithm is indeed much faster. Nevertheless, the memory occupation becomes more important since all the values of the sequence dW_n must be known simultaneously to calculate the Fourier transform, which limits the possibility of using this algorithm for large Reynolds numbers.

Such limitation can be overcome by using the approach proposed in Ref. [82] based on the inverse Laplace transform of the convolution kernel. In this approach Γ is estimated as a weighted sum of correlated Orstein-Uhlenbeck processes with characteristic time ranging from τ_c to τ_ε.

Despite its efficiency, neither this technique, nor the one based on FFT, can be used to determine the $\hat{\Gamma}$ that appears in the vectorial stochastic model for the acceleration, or as noted by Ref. [78]
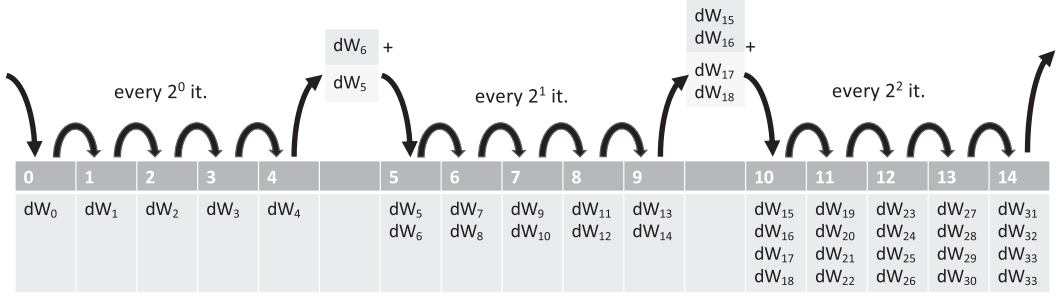
FIG. 18. Diagram illustrating the coarse-graining of the integral (D17) and the nonuniform update of the list.

for velocity gradients. Indeed, in such cases it is not the increments of the components of the Wiener process which are convoluted but a projection of them as shown in Eq. (48). The issue is that the projection cannot by computed *a priori*, because it requires knowing a_i and u_i, as seen in Eq. (49).

For these reasons we propose a new algorithm which is fast, using a limited amount of memory and which only requires knowing the dW_n sequentially. This algorithm is derived from the one introduced for nonstochastic integrals in Ref. [58]. As we go back in the past, we can afford to remember with less precision the noise entering this integral, since the kernel decreases with the lag. We will thus proceed by progressive "coarse graining" and group together the oldest dW_n, by introducing an increasingly extended local average. We then decompose the sum of Eq. (D20) into subsums comprising an increasing number of terms:

$$
\begin{aligned}
-2\Gamma_n &= \sum_{m=0}^{N_{\text{hist}}} (s_m + \tau_c)^{-3/2} dW_{n-m} \\
&= \sum_{m=m_{s1}}^{m_{e1}} (s_m + \tau_c)^{-3/2} dW_{n-m} + \cdots + \sum_{m=m_{sN}}^{m_{eN}} (s_m + \tau_c)^{-3/2} dW_{n-m} \\
&= \sum_{j=1}^{N} \sum_{m=m_{sj}}^{m_{ej}} (s_m + \tau_c)^{-3/2} dW_{n-m} \\
&\approx \sum_{j=1}^{N} (\bar{s}_j + \tau_c)^{-3/2} \overline{dW}_j,
\end{aligned}
\tag{D21}
$$

where we introduced $\bar{s}_j = (m_{ej} + m_{sj})dt/2$ and $\overline{dW}_j = \sum_{m=m_{sj}}^{m_{ej}} dW_{n-m}$ such that $(\bar{s}_j + \tau_c)^{-3/2} \overline{dW}_j \approx \sum_{m=m_{sj}}^{m_{ej}} (s_m + \tau_c)^{-3/2} dW_{n-m}$. The bounds m_{ej} and m_{sj} are progressively spaced as j increases leading to an increasingly coarse splitting of the integral. This approximation of the integral can be carried out very efficiently by using a nonhomogeneous list updating for $\overline{dW}$. The first elements of the list are updated every time steps and the older ones less and less regularly, as described in the diagram of Fig. 18. In detail, we update the first N_s elements of the list at each time step, the following N_s every two time steps, and the elements between iN_s and $(i + 1)N_s$ are only updated every 2^i iterations. Thus, with $n \times N_s$ elements in the list we can estimate the integral going up to $\sum_{i=0}^{n} N_s 2^i dt = 2N_s(2^n - 1)dt$ in the past. This gives a considerable saving in computation time and memory with good accuracy as it is illustrated in Fig. 17. For all the calculation presented in this paper we have used $N_s = 12$.

[1] A. La Porta, G. A. Voth, A. M. Crawford, J. Alexander, and E. Bodenschatz, Fluid particle accelerations in fully developed turbulence, Nature **409**, 1017 (2001).

[2] N. Mordant, A. M. Crawford, and E. Bodenschatz, Experimental Lagrangian acceleration probability density function measurement, Physica D: Nonlinear Phenom. **193**, 245 (2004).

[3] N. Mordant, A. M. Crawford, and E. Bodenschatz, Three-Dimensional Structure of the Lagrangian Acceleration in Turbulent Flows, Phys. Rev. Lett. **93**, 214501 (2004).

[4] G. A. Voth, A. La Porta, A. M. Grawford, J. Alexander, and E. Bodenschatz, Measurements of particle accelerations in fully developed turbulence, J. Fluid Mech. **469**, 121 (2002).

[5] N. Mordant, J. Delour, E. Lévêque, A. Arnéodo, and J.-F. Pinton, Long Time Correlations in Lagrangian Dynamics: A Key to Intermittency in Turbulence, Phys. Rev. Lett. **89**, 254502 (2002).

[6] N. Mordant, E. Lévêque, and J.-F. Pinton, Experimental and numerical study of the Lagrangian dynamics of high Reynolds turbulence, New J. Phys. **6**, 116 (2004).

[7] S. B. Pope, Lagrangian microscales in turbulence, Philos. Trans. R. Soc. London A **333**, 309 (1990).

[8] L. Biferale, G. Boffetta, A. Celani, A. Lanotte, and F. Toschi, Particle trapping in three-dimensional fully developed turbulence, Phys. Fluids **17**, 021701 (2005).

[9] L. Biferale and F. Toschi, Joint statistics of acceleration and vorticity in fully developed turbulence, J. Turbul. **6**, N40 (2006).

[10] H. Homann, D. Schulz, and R. Grauer, Conditional Eulerian and Lagrangian velocity increment statistics of fully developed turbulent flow, Phys. Fluids **23**, 055102 (2011).

[11] A. M. Reynolds, N. Mordant, A. M. Crawford, and E. Bodenschatz, On the distribution of Lagrangian accelerations in turbulent flows, New J. Phys. **7**, 58 (2005).

[12] P. K. Yeung, S. B. Pope, A. G. Lamorgese, and D. A. Donzis, Acceleration and dissipation statistics of numerically simulated isotropic turbulence, Phys. Fluids **18**, 065103 (2006).

[13] A. K. Aringazin and M. I. Mazhitov, stochastic models of Lagrangian acceleration of fluid particle in developed turbulence, Int. J. Mod. Phys. B **18**, 3095 (2004).

[14] L. Biferale, G. Boffetta, A. Celani, B. J. Devenish, A. Lanotte, and F. Toschi, Multifractal Statistics of Lagrangian Velocity and Acceleration in Turbulence, Phys. Rev. Lett. **93**, 064502 (2004).

[15] M. S. Borgas and P. K. Yeung, Conditional fluid-particle accelerations in turbulence, Theor. Comput. Fluid Dyn. **11**, 69 (1998).

[16] A. M. Crawford, N. Mordant, and E. Bodenschatz, Joint Statistics of the Lagrangian Acceleration and Velocity in Fully Developed Turbulence, Phys. Rev. Lett. **94**, 024501 (2005).

[17] B. L. Sawford, P. K. Yeung, M. S. Borgas, P. Vedula, A. La Porta, A. M. Crawford, and E. Bodenschatz, Conditional and unconditional acceleration statistics in turbulence, Phys. Fluids **15**, 3478 (2003).

[18] A. Tsinober, *An Informal Conceptual Introduction to Turbulence*, 2nd ed. (Springer, Berlin, 2009).

[19] A. Arnèodo, R. Benzi, J. Berg, L. Biferale, E. Bodenschatz, A. Busse, E. Calzavarini, B. Castaing, M. Cencini, L. Chevillard, R. T. Fisher, R. Grauer, H. Homann, D. Lamb, A. S. Lanotte, E. Lévêque, B. Luthi, J. Mann, N. Mordant, W.-C. Muller, S. Ott, N. T. Ouellette, J.-F. Pinton, S. B. Pope, S. G. Roux, F. Toschi, H. Xu, and P. K. Yeung, Universal Intermittent Properties of Particle Trajectories in Highly Turbulent Flows, Phys. Rev. Lett. **100**, 254504 (2008).

[20] L. Biferale, E. Bodenschatz, M. Cencini, A. S. Lanotte, N. T. Ouellette, F. Toschi, and H. Xu, Lagrangian structure functions in turbulence: A quantitative comparison between experiment and direct numerical simulation, Phys. Fluids **20**, 065103 (2008).

[21] L. Chevillard, S. G. Roux, E. Levêque, N. Mordant, J.-F. Pinton, and A. Arneodo, Lagrangian Velocity Statistics in Turbulent Flows: Effects of Dissipation, Phys. Rev. Lett. **91**, 214502 (2003).

[22] A. S. Lanotte, L. Biferale, G. Boffetta, and F. Toschi, A new assessment of the second-order moment of Lagrangian velocity increments in turbulence, J. Turbul. **14**, 34 (2013).

[23] B. L. Sawford and P. K. Yeung, Turbulent Lagrangian velocity statistics conditioned on extreme values of dissipation, Procedia IUTAM **9**, 129 (2013).

[24] T. D. Drivas, Turbulent cascade direction and Lagrangian time-asymmetry, J. Nonlinear Sci. **29**, 65 (2019).

[25] B. Dubrulle, Beyond Kolmogorov cascades, J. Fluid Mech. **867**, P1 (2019).

[26] G. Falkovich, H. Xu, A. Pumir, E. Bodenschatz, L. Biferale, G. Boffetta, A. S. Lanotte, and F. Toschi, On Lagrangian single-particle statistics, Phys. Fluids **24**, 055102 (2012).

[27] A. Pumir, H. Xu, G. Boffetta, G. Falkovich, and E. Bodenschatz, Redistribution of Kinetic Energy in Turbulent Flows, Phys. Rev. X **4**, 041006 (2014).

[28] H. Xu, A. Pumir, G. Falkovich, E. Bodenschatz, M. Shats, H. Xia, N. Francois, and G. Boffetta, Flight-crash events in turbulence, Proc. Natl. Acad. Sci. USA **111**, 7558 (2014).

[29] S. Douady, Y. Couder, and M. E. Brachet, Direct Observation of the Intermittency of Intense Vorticity Filaments in Turbulence, Phys. Rev. Lett. **67**, 983 (1991).

[30] A. Tsinober, P. Vedula, and P. K. Yeung, Random taylor hypothesis and the behavior of local and convective accelerations in isotropic turbulence, Phys. Fluids **13**, 1974 (2001).

[31] A. Chorin, *Vorticity and Turbulence* (Springer, Berlin, 1994).

[32] P. Constantin and G. Iyer, A stochastic Lagrangian representation of the three-dimensional incompressible Navier–Stokes equations, Commun. Pure Appl. Math. **61**, 330 (2008).

[33] C. S. Peskin, A random-walk interpretation of the incompressible Navier-Stokes equations, Commun. Pure Appl. Math. **38**, 845 (1985).

[34] A. N. Kolmogorov, The local structure of turbulence in incompressible viscous fluid for very large Reynolds numbers, Dokl. Akad. Nauk SSSR **30**, 301 (1941).

[35] A. N. Kolmogorov, A refinement of previous hypotheses concerning the local structure of turbulence in a viscous incompressible fluid at high Reynolds number, J. Fluid Mech. **13**, 82 (1962).

[36] W. J. T. Bos and R. Zamansky, Power Fluctuations in Turbulence, Phys. Rev. Lett. **122**, 124504 (2019).

[37] J. M. Lawson, E. Bodenschatz, A. N. Knutsen, J. R. Dawson, and N. A. Worth, Direct assessment of Kolmogorov's first refined similarity hypothesis, Phys. Rev. Fluids **4**, 022601 (2019).

[38] S. Tang, R. Antonia, L. Djenidi, and Y. Zhou, Scaling of the turbulent energy dissipation correlation function, J. Fluid Mech. **891**, A26 (2020).

[39] B. L. Sawford, Reynolds number effects in Lagrangian stochastic models of turbulent dispersion, Phys. Fluids A: Fluid Dyn. **3**, 1577 (1991).

[40] S. B. Pope and Y. L. Chen, The velocity-dissipation probability density function model for turbulent flows, Phys. Fluids **2**, 1437 (1990).

[41] C. Beck, Lagrangian acceleration statistics in turbulent flows, Europhys. Lett. **64**, 151 (2003).

[42] A. M. Reynolds, On the application of nonextensive statistics to Lagrangian turbulence, Phys. Fluids **15**, L1 (2003).

[43] A. M. Reynolds, Superstatistical Mechanics of Tracer-Particle Motions in Turbulence, Phys. Rev. Lett. **91**, 084503 (2003).

[44] A. G. Lamorgese, S. B. Pope, P. K. Yeung, and B. L. Sawford, A conditionally cubic-Gaussian stochastic Lagrangian model for acceleration in isotropic turbulence, J. Fluid Mech. **582**, 423 (2007).

[45] A. M. Reynolds, K. Yeo, and C. Lee, Anisotropy of Acceleration in Turbulent Flows **70**, 017302 (2004).

[46] B. Viggiano, J. Friedrich, R. Volk, M. Bourgoin, R. B. Cal, and L. Chevillard, Modelling Lagrangian velocity and acceleration in turbulent flows as infinitely differentiable stochastic processes, J. Fluid Mech. **900**, A27 (2020).

[47] E. Bacry, J. Delour, and J. F. Muzy, Multifractal random walk, Phys. Rev. E **64**, 026103 (2001).

[48] J.-P. Kahane and J. Peyrière, Sur certaines martingales de Benoit Mandelbrot, Adv. Math. **22**, 131 (1976).

[49] B. B. Mandelbrot, Intermittent turbulence in self-similar cascades: Divergence of high moments and dimension of the carrier, J. Fluid Mech. **62**, 331 (1974).

[50] A. M. Reynolds, Superstatistical Lagrangian stochastic modeling, Physica A **340**, 298 (2004).

[51] S. B. Pope, A stochastic Lagrangian model for acceleration in turbulent flows, Phys. Fluids **14**, 2360 (2002).

[52] A. Barge and M. A. Gorokhovski, Acceleration of small heavy particles in homogeneous shear flow: Direct numerical simulation and stochastic modelling of under-resolved intermittent turbulence, J. Fluid Mech. **892**, A28 (2020).

[53] M. Gorokhovski and S. K. Oruganti, Stochastic models for the droplet motion and evaporation in under-resolved turbulent flows at a large Reynolds number, J. Fluid Mech. **932**, A18 (2022).

[54] M. Gorokhovski and R. Zamansky, Modeling the effects of small turbulent scales on the drag force for particles below and above the Kolmogorov scale, Phys. Rev. Fluids **3**, 034602 (2018).

[55] V. Sabelnikov, A. Barge, and M. Gorokhovski, Stochastic modeling of fluid acceleration on residual scales and dynamics of suspended inertial particles in turbulence, Phys. Rev. Fluids **4**, 044301 (2019).

[56] V. Sabel'nikov, A. Chtab-Desportes, and M. Gorokhovski, New subgrid stochastic acceleration model in LES of high-Reynolds-number flows, Eur. Phys. J. B **80**, 177 (2011).

[57] Z. Zhang, D. Legendre, and R. Zamansky, Model for the dynamics of micro-bubbles in high Reynolds number flows, J. Fluid Mech. **879**, 554 (2019).

[58] F. Le Roy De Bonneville, R. Zamansky, F. Risso, A. Boulin, and J.-F. Haquet, Numerical simulations of the agitation generated by coarse-grained bubbles moving at large Reynolds number, J. Fluid Mech. **926**, A20 (2021).

[59] R. Zamansky, F. Coletti, M. Massot, and A. Mani, Turbulent thermal convection driven by heated inertial particles, J. Fluid Mech. **809**, 390 (2016).

[60] B. Kumar, J. Schumacher, and R. A. Shaw, Lagrangian mixing dynamics at the cloudy–clear air interface, J. Atmos. Sci. **71**, 2564 (2014).

[61] J. Bec, L. Biferale, M. Cencini, A. Lanotte, and F. Toschi, Intermittency in the velocity distribution of heavy particles in turbulence, J. Fluid Mech. **646**, 527 (2010).

[62] A. Lanotte, E. Calzavarini, T. Federico, B. Jeremie, B. Luca, and C. Massimo, Heavy particles in turbulent flows, International CFD Database (2011), doi: 10.4121/uuid:a64319d5-1735-4bf1-944b-8e9187e4b9d6

[63] G. I. Barenblatt, *Scaling* (Cambridge University Press, Cambridge, UK, 2002).

[64] G. I. Barenblatt and A. J. Chorin, New perspectives in turbulence: Scaling laws, asymptotics, and intermittency, SIAM Rev. **40**, 265 (1998).

[65] G. I. Barenblatt and A. J. Chorin, A mathematical model for the scaling of turbulence, Proc. Natl. Acad. Sci. USA **101**, 15023 (2004).

[66] B. Castaing, Y. Gagne, and M. Marchand, Log-similarity for turbulent flows? Physica D: Nonlinear Phenom. **68**, 387 (1993).

[67] Y. Gagne and B. Castaing, Une représentation universelle sans invariance globale d'échelle des spectres d'énergie en turbulence développée, C. R. Acad. Sci. **312**, 441 (1991).

[68] R. J. Hill, Scaling of acceleration in locally isotropic turbulence, J. Fluid Mech. **452**, 361 (2002).

[69] A. M. Oboukhov, Some specific features of atmospheric turbulence, J. Fluid Mech. **13**, 77 (1962).

[70] B. Castaing, Y. Gagne, and E. J. Hopfinger, Velocity probability density functions of high Reynolds number turbulence, Physica D: Nonlin. Phenom. **46**, 177 (1990).

[71] R. Benzi, G. Paladin, G. Parisi, and A. Vulpiani, On the multifractal nature of fully developed turbulence and chaotic systems, J. Phys. A: Math. Gen. **17**, 3521 (1984).

[72] U. Frisch, P.-L. Sulem, and M. Nelkin, A simple dynamical model of intermittent fully developed turbulence, J. Fluid Mech. **87**, 719 (1978).

[73] A. N. Kolmogorov, On the log-normal distribution of particles sizes during break-up process, Dokl. Akad. Nauk SSSR **31**, 99 (1941).

[74] A. S. Monin and A. M. Yaglom, *Statistical Fluid Mechanics: Mechanics of Turbulence*, Vol. 2 (MIT Press, Cambridge, MA, 1981).

[75] A. M. Yaglom, The influence of fluctuations in energy dissipation on the shape of turbulence characteristics in the inertial interval, Sov. Phys. Dokl. **11**, 26 (1966).

[76] J. R. Picardo, A. Bhatnagar, and S. S. Ray, Lagrangian irreversibility and Eulerian dissipation in fully developed turbulence, Phys. Rev. Fluids **5**, 042601(R) (2020).

[77] S. S. Girimaji and S. B. Pope, A diffusion model for velocity gradients in turbulence, Phys. Fluids A: Fluid Dyn. **2**, 242 (1990).

[78] R. M. Pereira, L. Moriconi, and L. Chevillard, A multifractal model for the velocity gradient dynamics in turbulent flows, J. Fluid Mech. **839**, 430 (2018).

[79] R. Zamansky, I. Vinkovic, and M. Gorokhovski, Acceleration in turbulent channel flow: Universalities in statistics, subgrid stochastic models and an application, J. Fluid Mech. **721**, 627 (2013).

[80] M. Wilkinson and A. Pumir, Spherical Ornstein-Uhlenbeck processes, J. Stat. Phys. **145**, 113 (2011).

[81] L. Chevillard, Regularized fractional Ornstein-Uhlenbeck processes and their relevance to the modeling of fluid turbulence, Phys. Rev. E **96**, 033111 (2017).

[82] R. Letournel, L. Goudenège, R. Zamansky, A. Vié, and M. Massot, Reexamining the framework for intermittency in Lagrangian stochastic models for turbulent flows: A way to an original and versatile numerical approach, Phys. Rev. E **104**, 015104 (2021).

[83] Benoit B. Mandelbrot and John W. Van Ness, Fractional Brownian motions, fractional noises, and applications, SIAM Rev. **10**, 422 (1968).

[84] J. F. Hackl, P. K. Yeung, and B. L. Sawford, Multi-particle and tetrad statistics in numerical simulations of turbulent relative dispersion, Phys. Fluids **23**, 065103 (2011).

[85] B. L. Sawford and P. K. Yeung, Kolmogorov similarity scaling for one-particle Lagrangian statistics, Phys. Fluids **23**, 091704 (2011).

[86] See Supplemental Material at http://link.aps.org/supplemental/10.1103/PhysRevFluids.7.084608 for a basic script in python presenting the algorithm to integrate the proposed stochastic model.

[87] H. Tennekes and J. L. Lumley, *A First Course in Turbulence* (MIT Press, Cambridge, MA, 1972).

[88] H. K. Moffat, Interaction of turbulence with strong wind shear, In *Atmosphere Turbulence and Radio Wave Propagation*, edited by A. M. Yaglom and V. I. Tatarsky (Nauka, Moscow, 1967), pp. 139–156.

[89] C. Lee, K. Yeo, and J.-I. Choi, Intermittent Nature of Acceleration in Near Wall Turbulence, Phys. Rev. Lett. **92**, 144502 (2004).

[90] C. W. Gardiner, *Handbook of Stochastic Methods for Physics, Chemistry and the Natural Sciences* (Springer, Berlin, 1985).

[91] A. Innocenti, N. Mordant, N. Stelzenmuller, and S. Chibbaro, Lagrangian stochastic modelling of acceleration in turbulent wall-bounded flows, J. Fluid Mech. **892**, A38 (2020).

[92] S. B. Pope, On the relationship between stochastic Lagrangian models of turbulence and second-moment closures, Phys. Fluids **6**, 973 (1994).

[93] Z. Zhang, D. Legendre, and R. Zamansky, Fluid inertia effects on the motion of small spherical bubbles or solid spheres in turbulent flows, J. Fluid Mech. **921**, A4 (2021).

[94] P. L. Johnson and C. Meneveau, A closure for Lagrangian velocity gradient evolution in turbulence using recent-deformation mapping of initially gaussian fields, J. Fluid Mech. **804**, 387 (2016).

[95] C. Meneveau, Lagrangian dynamics and models of the velocity gradient tensor in turbulent flows, Annu. Rev. Fluid Mech. **43**, 219 (2011).

[96] M. Wilczek, A. Daitche, and R. Friedrich, On the velocity distribution in homogeneous isotropic turbulence: Correlations and deviations from Gaussianity, J. Fluid Mech. **676**, 191 (2011).

[97] B. Castaing, The temperature of turbulent flows, J. Phys. II **6**, 105 (1996).

[98] B. B. Mandelbrot, Possible refinement of the log-normal hypothesis concerning the distribution of energy dissipation in intermittent turbulence, in *Statistical Models and Turbulence*, edited by M. Rosenblatt and C. Van Atta (Springer, Berlin, 1972), pp. 333–351.

[99] M. S. Borgas, The multifractal Lagrangian nature of turbulence, Philosophical Transactions: Physical Sciences and Engineering **342**, 379 (1993).

[100] Y. Huang and F. G. Schmitt, Lagrangian cascade in three-dimensional homogeneous and isotropic turbulence, J. Fluid Mech. **741**, R2 (2014).

[101] C. Meneveau and T. S. Lund, On the Lagrangian nature of the turbulence energy cascade, Phys. Fluids **6**, 2820 (1994).

[102] B. L. Sawford and P. K. Yeung, Direct numerical simulation studies of Lagrangian intermittency in turbulence, Phys. Fluids **27**, 065109 (2015).